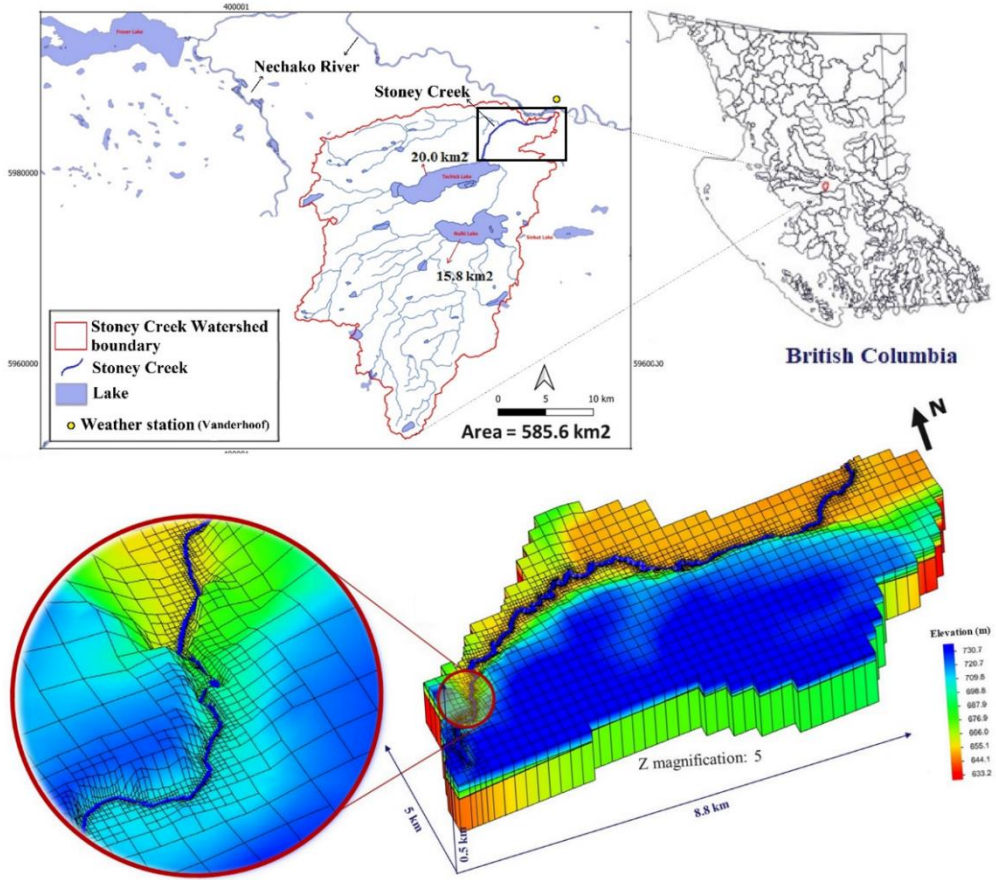# Impact of Cumulative Groundwater Withdrawal on Surface Water and Groundwater Interaction in the Stoney Creek Watershed

Davood Mahmoodzadeh, Jun Yin, and Jianbing Li

February 2025

The **Water Science Series** are scientific technical reports relating to the understanding and management of B.C.'s water resources. The series communicates scientific knowledge gained through water science programs across B.C. government, as well as scientific partners working in collaboration with provincial staff. For additional information visit: http://www2.gov.bc.ca/gov/content/environment/air-land-water/water/water-science-data/water-science-series.

Author's Affiliation:
Mahmoodzadeh Davood, Ph.D.
University of Northern British Columbia
3333 University Way, Prince George, BC V2N 4Z9

Jun Yin, Ph.D., PGeo.
Forest Improvement and Research Management Branch, Ministry of Forests
499 George St., Prince George, BC V2L 1R5

Jianbing Li, Ph.D., PEng.
University of Northern British Columbia
3333 University Way, Prince George, BC V2N 4Z9

Cover Photographs:
Stoney Creek in Vanderhoof, Davood Mahmoodzadeh

EXECUTIVE SUMMARY

In the present study, an integrated groundwater and surface water interaction (GSI) model was developed to account for the cumulative groundwater withdrawal effects on the Stoney Creek Watershed in British Columbia, Canada. A 3-D numerical model was created using the MODFLOW-USG code, with the modelling domain and aquifer hydraulic parameters defined based on a recent aquifer mapping project in the Vanderhoof area (Hinnell et al., 2020). The model employed a high-resolution Digital Elevation Model (DEM) to capture the river morphology and the heterogeneity of the local groundwater system. The model was calibrated for steady-state and transient conditions based on groundwater and Stoney Creek water level measurements collected from 2015 to 2017. Static groundwater level measurements recorded in GWELLS for wells in both unconfined and confined aquifers were also used in the model calibration. The model calibration parameters include the hydraulic conductivity of geologic units, streambed hydraulic conductivity, and infiltration coefficients. These parameters were calibrated using the automated parameter estimation model (PEST) and by trial-and-error methods. A sensitivity analysis was conducted to evaluate the influence of the main modelling parameters on simulations results. The calibrated model was used to assess the influence of different pumping, climate, and groundwater level scenarios on groundwater-surface water interaction in Stoney Creek. Finally, a risk map showing the influence of each pumping well on groundwater-surface water interaction and potential streamflow capture was prepared for current pumping conditions.

The base case simulation demonstrated that groundwater is an important source of streamflow in Stoney Creek. Groundwater contributions to the flow in Stoney Creek (Dg) was estimated to range from 0.01 to 23.6 million cubic meters per year (MCM/yr) at various stream reaches. The time series of simulated groundwater discharge demonstrated the highest contribution occurs from January to March 2015 when more than 2 MCM is provided to streamflow by the groundwater system. The sensitivity analysis of the model showed that among all the parameters, the riverbed hydraulic conductivity and the hydraulic conductivity of the confined aquifer had the highest and the lowest sensitivity, respectively. Specified head boundary conditions along the northern and southern boundaries of the model domain also significantly influenced the volume of groundwater discharge to Stoney Creek. A 2 m decline in groundwater levels along the northern boundary resulted in a 30% reduction in predicted groundwater discharge to Stoney Creek, compared to a 13% reduction for similar groundwater level decline along the southern boundary. The most sensitive and impacted stream sections in the model are near to the northern boundary, which indicates the need for more focused groundwater monitoring and management in the northern regions of the watershed.

The calibrated numerical model was used to investigate the impacts of different groundwater pumping scenarios on groundwater discharge. A 50% increase in groundwater pumping over current levels was found to reduce groundwater discharge by 0.6% in December 2018. In comparison, under dry conditions with only a 10% increase in groundwater use, the results showed a gradual decrease in groundwater discharge to 24.5 MCM by 2026, representing a 0.7% reduction compared to 2017. The results of cumulative groundwater withdrawal scenarios showed that groundwater discharge decreased by 7% in 2026 and decreased by 9% in 2035. Finally, the risk analysis and associated risk map shows wells classified as very high-risk are located in unconfined aquifers in close proximity to Stoney Creek and experience rapid water level changes due to groundwater withdrawal. The numerical results and risk map from this project can support decision-makers active in the water allocation sector who require detailed understanding the impacts of cumulative groundwater withdrawal on groundwater-surface water interactions in order to develop effective sustainable water management strategies and associated protection of aquatic ecosystem functions.

CONTENTS

FIGURES

TABLES

1. INTRODUCTION

Groundwater is currently a reliable water source for different purposes (domestic, industrial, and agricultural) in many watersheds of Canada such as in the Stoney Creek Watershed in Northern British Columbia (B.C.) (Figure 1). Furthermore, surface water bodies (rivers/streams, lakes, reservoirs, and wetlands) are frequently hydraulically connected to underlying groundwater resources. Interaction between surface water and groundwater occurs through the loss of surface water to groundwater, seepage of groundwater to surface water bodies, or a combination of both (Zhou and Li, 2011; Saha et al., 2017; Li et al., 2024). Stream reaches that gain water from the inflow of groundwater through the streambed are called gaining streams. For this to occur, the elevation of the groundwater level (piezometric head) must be higher than the level of the surface of the stream. Stream reaches that lose water to the groundwater system by outflow through the streambed are called losing streams (Cui et al., 2024). Moreover, streams can exhibit both gaining and losing characteristics on different reaches, and these interaction dynamics can vary seasonally based on precipitation patterns and the relative water levels of groundwater and surface water (Zaremehrjardy et al., 2022).

The Stoney Creek Watershed (SCW) is a sub-watershed of the Nechako River Watershed and includes the town of Vanderhoof and the Saik'uz First Nations Reserve in Northern B.C. In this watershed, shallow groundwater frequently interacts with surface water. Water withdrawal from Stoney Creek can potentially decrease groundwater levels, and vice-versa, groundwater withdrawal can reduce flows in Stoney Creek (Aghbelagh et al., 2018; Mahmoodzadeh et al., 2023, 2024). In many situations, the impact of groundwater withdrawal on surface water varies depending on factors such as pumping duration, pumping location and rate, pumping well depth, number of wells, the hydrogeologic setting, and the connectivity between the water resources. In particular, pumping wells sufficiently close to the stream can potentially affect the hydraulic gradient and the rate of water flow between aquifers and surface water systems. Wells that are far from streams and rivers can also reduce streamflow by intercepting and diverting groundwater that would have eventually discharged to the stream (Khan et al. 2019; Valett and Sheibley, 2009). Understanding the interactions between groundwater and Stoney Creek is crucial for decision-makers to develop effective policies, practical legislation, sustainable water resource allocation, and for overall management and sound policy making. Local water resource managers need an improved understanding of the connection between groundwater and surface water and the possible effects of future development on groundwater and surface water resources, as well as aquatic ecosystems.
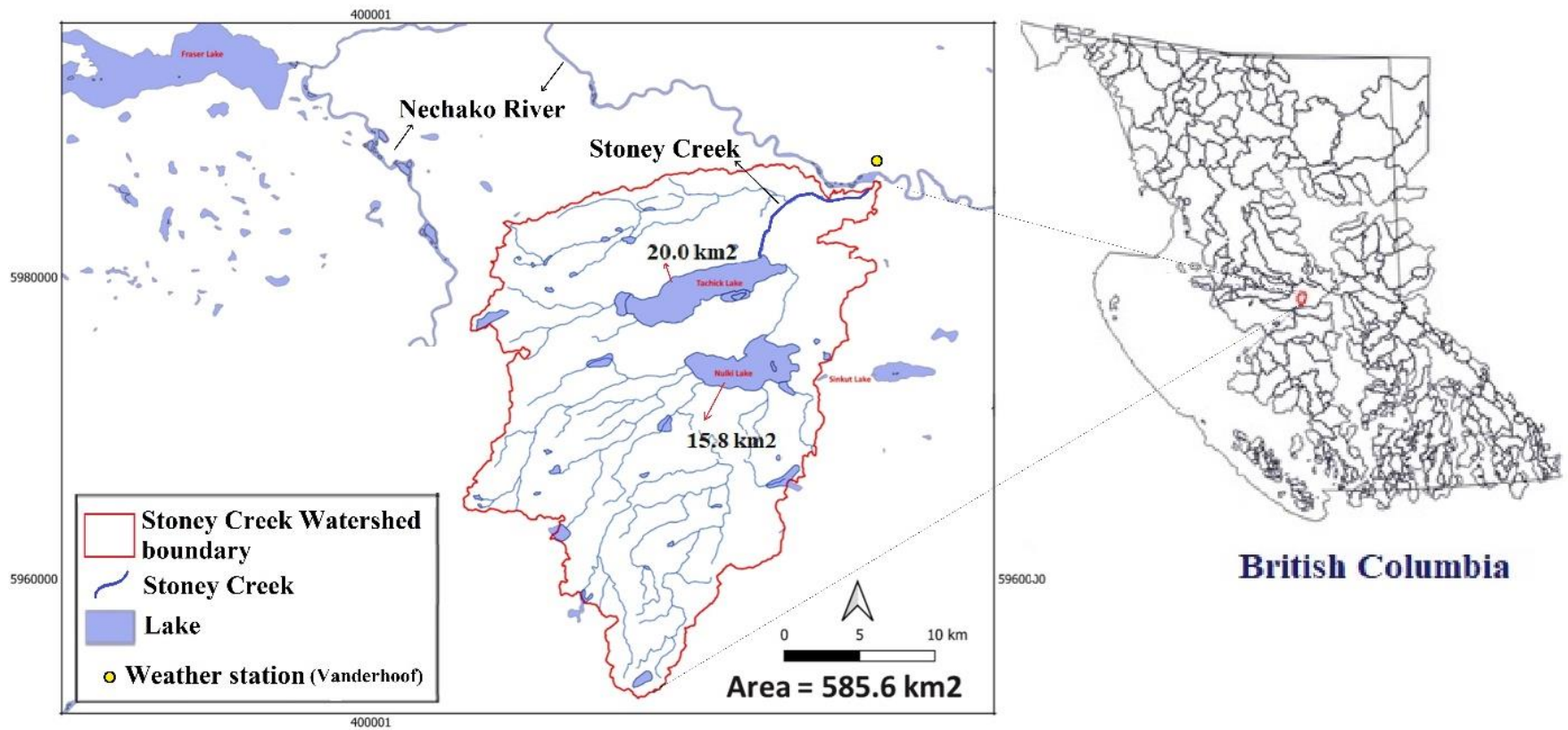
Figure 1. Stoney Creek Watershed in British Columbia, Canada.

2. PROJECT BACKGROUND AND LITERATURE REVIEW

A literature review of related investigations in the study area indicates that Aghbelagh et al. (2018) developed a transient groundwater flow model to examine groundwater and surface water interaction (GSI) in the SCW. The model was developed using the Visual MODFLOW program and was calibrated with observed groundwater and surface water levels data. The model results showed groundwater is a major contributor to the streamflow in Stoney Creek and the Nechako River in both wet and dry seasons. Although the numerical groundwater model was capable of simulating transient groundwater fluctuations and GSI, the project scope did not include an assessment of impacts from groundwater usage.

Various approaches and methods for quantifying GSIs and their advantages and disadvantages are summarized in Table 1. These approaches include hydraulic, temperature, geophysical, water budgets, remote sensing, hydrochemistry, and mathematical methods (Coluccio and Morgan, 2019; Hammett et al., 2022; Banerjee and Ganguly, 2023). Many of these studies employed multiple approaches and methods to meet their objectives. Among all methods, numerical models have been frequently used to simulate groundwater flow conditions and hydraulic connectivity as a complement to field measurements (e.g., Tran et al., 2020; Lambert et al., 2011; Deb et al., 2019; Waseem et al., 2020; Ghysels et al., 2021; Jafari et al., 2021).

Numerical models described in the literature range from simple conceptual frameworks to increasingly complex models that integrate key temporal and spatial processes, providing a more accurate representation of the physical system. For example, a transient model could be calibrated using specific field observations and data from local water authority experts to estimate the groundwater and GSI response to water allocation (Banerjee and Ganguly, 2023). Additionally, numerical simulation methods facilitate the modelling of heterogeneous, anisotropic hydrogeological systems and boundary conditions using irregular three-dimensional (3-D) geometries, allowing maximum flexibility and versatility (Chow et al., 2016; Banerjee and Granguly, 2023).

Many factors affect GSI, including, but not limited to, groundwater withdrawal, climate change, land use changes, and river morphology (Karki et al., 2021; Fang et al., 2024; Ketabchi et al., 2024). As a result of these combined effects, resource managers face challenges in understanding and quantifying man-made influences on GSI (e.g., pumping, climate change) needed for sustainable water resource management. Many previous studies consider and account for these factors in order to better quantify groundwater-surface water interactions (e.g., Ayenew et al., 2008; Sanz et al., 2011; May and Mazlan, 2014; Balbarini et al., 2017; Zhou et al., 2018; Bailey et al., 2020 and 2021; Singh and Ghosh, 2022; Zhou et al., 2023; Fang et al., 2024; Han et al., 2024).

Han et al. (2024) investigated a regional scale 3-D groundwater flow model covering several recognized surface water basins. In their study, groundwater withdrawal and river morphology factors were not considered in the interaction conceptualization. Fang et al. (2024) developed a meshless model to simulate variably saturated groundwater flow, including the effects of pumping/injection wells. Their study emphasized that by conceptualizing the detailed processes into governing equations, a numerical model can effectively simulate a broad range of real-world problems, making it a useful tool for groundwater resource decision-making. However, their simulation results are also affected by simplifications and assumptions such as a homogeneous aquifer (e.g., Balbarini et al.,2017; Tran et al., 2020; Gebere et al., 2021; Zhou et al., 2023).

Table 1. Approaches and methods for measuring groundwater and surface water interactions (source: Coluccio and Morgan, 2019; Hammett et al., 2022; Banerjee and Ganguly, 2023).

Approaches	Methods	Overall mechanism	Advantages	Disadvantages	Applications of these methods
Water budgets	• Surface water and groundwater budget calculation	Estimating inflow and outflow for groundwater and surface water systems	• Conceptually simple • Suitable for large regional-scale studies and homogenous aquifers	• Data limitations can be significant • Results are static in time • Cannot be used to forecast GSI response to pumping	Larned et al. (2015); Kebede et al. (2021); Li et al. (2020)
Hydrochemistry	• Injected tracer tests and environmental tracer tests (isotopes)	Quantifying chemical ions in water samples; using tracer injections to determine discharge	• Better estimation of large-scale interactions • Effective with significantly different isotope concentrations	• Isotope concentration variability over time and space • Less useful if isotope concentration differences are too small to quantify • Tracer characteristics may impact quantification and influence biogeochemical processes in the water	Zlotnik et al. (2016); Longa and Koontanakulvong (2020); Navarro-Martínez et al. (2020)
Temperature	• Vertical bed temperature profiling, • Spatial bed temperature mapping • Paired air and water temperature logging	Relating the difference in the temperature between groundwater and surface water	• Discharge and recharge can be differentiated while quantifying water flux • Relatively easy and fast data collection with sensors and probes	• Data accuracy depends on the instruments used • May be costly depending on the measurement method • Data collection is required across various locations • A significant temperature difference between sources is necessary for accurate quantification of GSI	Coluccio (2018); Thomas (2021); Sadat-Noori et al. (2021)

Table 1 continued. Approaches and methods for measuring groundwater and surface water interactions.

Approaches	Methods	Overall mechanism	Advantages	Disadvantages	Applications of these methods
Mathematical modelling	• Analytical solutions • Semi analytical solutions • Numerical model (MODFLOW, SWAT-MODFLOW, etc.)	Solving the governing equations of groundwater flow under different conditions and simplifying assumptions to represent the actual scenario	• Widely applicable to a range of hydrologic and geologic conditions • Can be used for very complex phenomena • Applicable to both small- and large-scale studies	• Model development may require significant time and effort • Substantial computational resources may be required • Data requirements can be substantial and limiting • Various assumptions may be required that do not reflect actual conditions	Tran et al. (2020); Lambert et al. (2011); Deb et al. (2019); Waseem et al. (2020); Ghysels et al. (2021); Jafari et al. (2021); Karamouz et al. (2020)
Hydraulic	• Darcy fluxes • Physical and chemical hydrograph separation • Seepage meters	(1) Measure hydraulic gradient and hydraulic conductivity to obtain flow, (2) base flow component of stream flow at the outflow point of a watershed	• Wells can be installed in-stream or stream banks • Applicable to both small- and large-scale studies	• Deep groundwater wells are expensive to install, and measurements must be taken at the same time • Need long term daily steam flow, specific discharge, and specific conductance	Sadat-Noori et al. (2021); Rau et al. (2019); Foks et al. (2019); Rumsey et al. (2020)
Remote sensing	• Lidar digital elevation mapping • multi- and hyperspectral imaging cameras	(1) Measure surface topography at high resolution, (2) measure specific electromagnetic spectrum wavelength bands	• Applicable to both small- and large-scale studies • Vegetation vigor can indicate near surface preferential GWI	• High-cost level and dependent on specific instrument/method used • The methods are not available for all locations	Briggs et al. (2019); Jackson (2020); Moore et al. (2020)
Geophysical	• Ground penetrating radar • electromagnetic induction continuous seismic profiling, and seismic refraction	Measure electrical resistivity by observing transient decay of induced electromagnetic currents in subsurface material	• Low-cost relative to groundwater monitoring • Dependent on specific instrument/methods used • Applicable to both small- and large-scale studies	• Surveys can be conducted over fresh-water environment • The depth of exploration is limited	Baawaain et al. (2018); Lane et al. (2020)

The resolution of Digital Elevation Models (DEMs) is another crucial factor that influences the extraction of key hydrological features such as river morphology (Mohtashami et al., 2022). Balbarini et al. (2017) developed a 3-D groundwater flow model to investigate the impact of river morphology on groundwater discharge to streams in an unconfined and homogenous sandy aquifer. The results showed that presence of meander bends leads to significant spatial variability in groundwater discharge. Lidberg et al. (2017) evaluated different pre-processing methods on LiDAR-based DEMs with different resolutions (2 m to 16 m) and showed that higher DEM resolution leads to more accurate stream network extractions. Also, Kasahara and Wondzell (2023) found that channel morphologic features strongly control hyporheic exchange flow in terms of GSI, with these controls varying based on stream size and channel constraint across four mountain stream reaches.

Previous studies have not used LiDAR-based DEM data to support development of GSI numerical models. For small rivers and creeks, the spacing between monitoring locations can be effectively captured in high-resolution DEMs, which allows for refined modelling grids along the river or creek. This also enables greater and more precise use of water level measurement data (from piezometers and stilling wells in the stream and along the banks) during the model calibration process, resulting in the development of a more accurate numerical model. Additionally, in most of the reviewed studies, the modelling domain was simplified by assuming homogeneous aquifer properties. In this study, we recognize that the heterogeneity of aquifers and the resolution of the DEM, in addition to groundwater withdrawal, are key processes and factors that must be considered for the development of a reliable GSI model (May and Mazlan, 2014; Zhou et al., 2018; Joo and Tian, 2021; Mahmoodzadeh and Karamouz, 2022). Further details of recent published numerical simulation studies of GSI are listed in Table 2. This table summarizes key features of previous studies including the study location, the simulation characteristics, aquifer hydrogeological properties, calibration and validation period, and other main factors considered in the simulation of GSI.

3. PROJECT OBJECTIVE

In this study, we focused on developing an integrated GSI model that accounts for the cumulative groundwater pumping effects, river morphology using high-resolution DEM, and the heterogeneity of the aquifers. Previous groundwater and surface water level measurements in the watershed (2015-2017) are used to calibrate the model. The research question of this project is to understand how groundwater withdrawals can change the magnitude of GSI in a heterogeneous environment. A 3-D numerical model is developed using the MODFLOW-USG code, and the modelling domain and aquifer hydraulic parameters are defined based on a recently completed aquifer mapping project in the Vanderhoof area (Hinnell et al., 2020). This report documents the development of the conceptual and numerical models of groundwater flow and GSI in the SCW. The report also describes the application of this model to estimate the groundwater contribution to Stoney Creek and the potential amount streamflow depletion resulting from cumulative groundwater withdrawals. The identification of cumulative impacts is important for making water allocation decisions. The results and tools from this research can support and inform groundwater allocation decisions in the SCW.

Table 2. Summary of the reviewed studies on numerical simulation of groundwater and surface water interaction.

Reference	Application Area (km²)	Simulation Characteristics [a]	Aquifer Hydrogeological Properties [b]	Calibration and Validation period	Main Factors Considered [c]			
					GWP	CC	LU	RM
Ayenew et al. (2008)	Akaki catchment, Ethiopia, (1462)	3-D, UNCO, SS, NU (MODFLOW)	HET, TL	Yes	✓	✗	✗	✗
Lambert et al. (2011)	Uinta River, USA, (-)	2-D, UNCO, TR NU (MODFLOW)	HM	Yes (2008-2009)	✓	✗	✗	✗
Sanz et al. (2011)	Mancha Oriental, Spain, (7260)	3-D, CO, UNCO, TR, NU (MODFLOW)	HET, ML	Yes (1982–2005)	✓	✗	✗	✗
May and Mazlan (2014)	Langat River, Malaysia, (243.65)	3-D, UNCO, SS, NU (MODFLOW)	HET, ML	Yes	✓	✗	✗	✗
Balbarini et al. (2017)	Grindsted stream, Denmark, (200)	3-D, UNCO, TR, NU	HM	Yes (2013-2014)	✗	✗	✓	✓
Zhou et al. (2018)	Schwarzbach River, Germany, (-)	2-D, UNCO, TR, NU, (MODFLOW)	HET	Yes (Aug 2010 to Oct 2010)	✗	✗	✗	✓
Aghbelagh et al. (2018)	Stoney Creek Canada, (155.6)	2-D, UNCO, TR, NU, (MODFLOW)	HET, TL	Yes (2015 to 2017)	✗	✗	✗	✗
Tran et al. (2020)	Pingtung Plain, Taiwan, (1300)	2-D, UNCO, TR, NU, (GSFLOW)	HOM	Yes (2015 to 2017)	✓	✗	✗	✗
Bailey et al. (2020)	Bosque River, USA, (470)	2-D, UNCO, TR, NU, (SWAT/ MODFLOW)	HET, ML	1993 to 2012	✗	✗	✗	✓
Bailey et al. (2021)	Price, Bosque and Animas Rivers, USA, (470, 3543, 4886)	2-D, UNCO, TR, NU, (MODFLOWNWT/A PEX)	HOM and HET	Yes (1992–1996, 2001–2009, and 1993–2000)	✗	✗	✗	✓

[a] 2-D: two-dimensional; 3-D: three-dimensional; UNCO: unconfined; CO: confined; SS: steady-state; TR: transient; NU: numerical; AN: analytical; GSFLOW: Surface- water flow; HEIFLOW: hydrological-ecological integrated watershed-scale flow.

[b] HOM: homogenous; HET: heterogeneous; TL: two-layer; ML: multi-layer.

[c] GWP: groundwater pumping/withdrawal; CC: climate change; F: flood; LU: land use change; RM: river morphology (using high resolution DEM).

Table 2 continued. Summary of the reviewed studies on numerical simulation of groundwater and surface water interaction.

Reference	Application Area (km^2)	Simulation Characteristics [a]	Aquifer Hydrogeological Properties [b]	Calibration and Validation period	Main Factors Considered [c]			
					GWP	CC	LU	RM
Joo and Tian (2021)	Geum River, Korea, (1800)	3-D, UNCO, TR, NU (HEIFLOW and GSFLOW)	HET, ML	Yes (2013)	✗	✓(F)	✗	✗
Gebere et al. (2021)	Modjo River, Ethiopia, (-)	2-D, UNCO, SS, NU (MODFLOW)	HOM	Yes	✓	✗	✓	✗
Singh and Ghosh (2022)	Cachar district, India, (3786)	2-D, UNCO, SS, NU (MODFLOW)	HET, TL	Yes (2006 to 2020)	✗	✗	✓	✗
Zhou et al. (2023)	Walnut Creek, USA	2-D, CO, UNCO, TR AN, NU (COMSOL)	HOM	Yes (-)	✗	✓(F)	✗	✗
Fang et al. (2024)	Hypothetical, (0.04); Mississippi, USA (-)	3-D, CO, UNCO, TR, NU (CCHE3-D-GW-Meshless)	HOM	Yes (2021)	✓	✗	✗	✗

[a] 2-D: two-dimensional; 3-D: three-dimensional; UNCO: unconfined; CO: confined; SS: steady-state; TR: transient; NU: numerical; AN: analytical; GSFLOW: Surface- water flow; HEIFLOW: hydrological-ecological integrated watershed-scale flow.

[b] HOM: homogenous; HET: heterogeneous; TL: two-layer; ML: multi-layer.

[c] GWP: groundwater pumping/withdrawal; CC: climate change; F: flood; LU: land use change; RM: river morphology (using high resolution DEM).

4. STUDY AREA

The location of the study area is shown in Figure 2. Stoney Creek begins at the outlet of Nulki Lake, flowing approximately 14 km northward through various agricultural, forested, and residential landscapes before reaching its confluence with Nechako River at the Migratory Bird Sanctuary in Vanderhoof. Model development in this study focused on the lower reach of the Stoney Creek (below Tachick Lake) mainly due to data availability and access to sites for field measurements and data collection. The modelling domain and numerical model development are discussed in Section 5.1.

4.1 Data Collection

Table 3 shows the source of data and information used in the conceptual and numerical model development. Criteria and procedures for determining the modelling domain in the study area and constructing numerical model are discussed in section 5.1 below.

Table 3. Inventory of data and information used in model development.

Data	Spatial scale	Source
Meteorological/climate	SCW	Pacific climate data[1]
Hydrometric stations	SCW	Real time hydrometric data[2]
Surface water uses	SCW	BC data catalogue[3]
Groundwater uses (well locations and volume of extraction)	SWC and Vanderhoof	
Water consumption type-contribution (Agricultural, industrial and domestic)	SWC or Vanderhoof	
Observation wells (GW level/depth measurements)	Vanderhoof	Groundwater level data provincial groundwater observation well network[4]
Pumping test data (Transmissivity, hydraulic conductivity, and specific storage)	Vanderhoof	
Aquifer layers, geologic information, and well lithology	SCW and Vanderhoof	GWELLS[5] and Hinnell et al. (2020)
Topographical map	SCW	GeoBC[6] and LiDAR[7]
Land use and land cover map	SCW	Sentinel-2, 10-m Land Use/Land Cover[8]
Pumping wells depth/level data	Vanderhoof	GWELLS[5]
Base layers including (1) watershed and sub watershed boundaries, aquifer, (2) surface water bodies, (3) names and locations of cities, states, political boundaries	SCW and Vanderhoof	

[1] https://www.pacificclimate.org/data
[2] https://wateroffice.ec.gc.ca
[3] https://owt.bcwatertool.ca/ watershed
[4] https://governmentofbc.maps.arcgis.com/
[5] https://apps.nrs.gov.bc.ca/gwells/
[6] https://www2.gov.bc.ca/gov/content/data/about-data-management/geobc
[7] https://lidar.gov.bc.ca/
[8] https://livingatlas.arcgis.com/landcover/
(All links accessed November 2024)
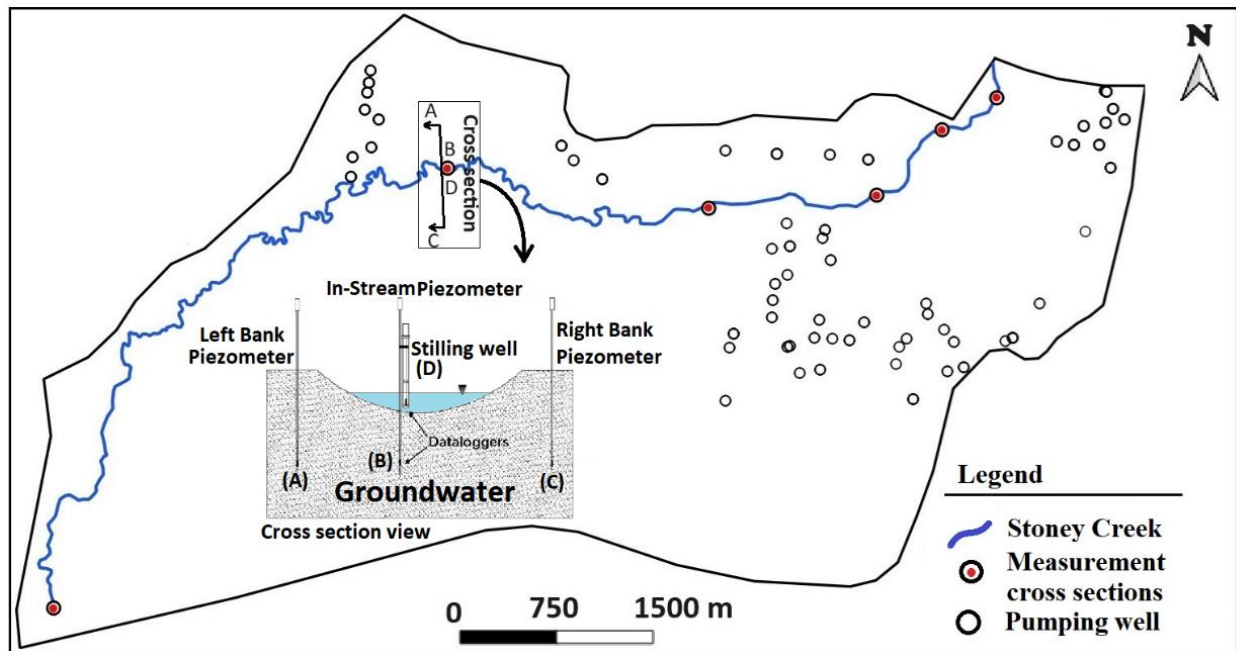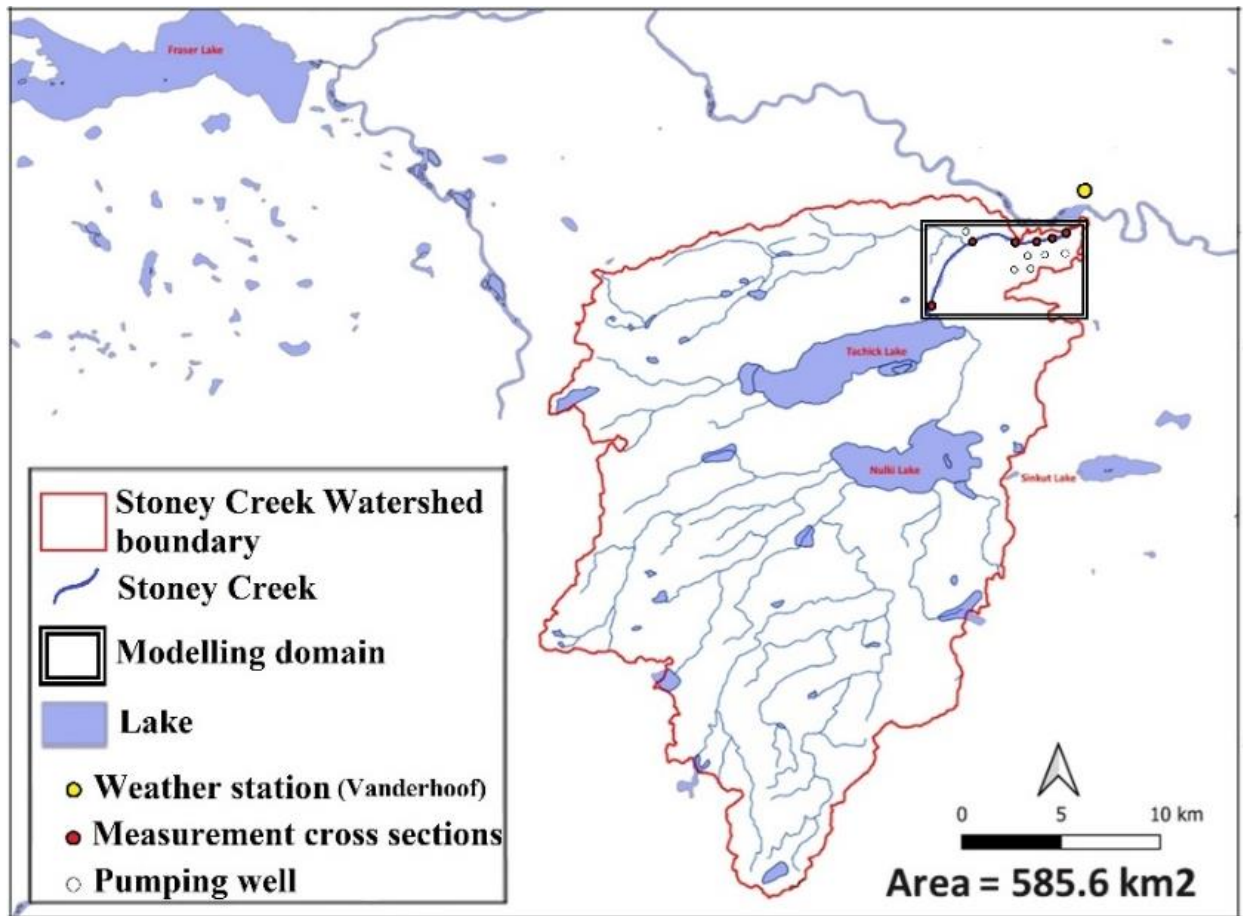
Figure 2. Location of the modelling domain within the Stoney Creek watershed (top) and the modelling domain showing the location of measurement cross sections and pumping wells (bottom).

4.2 Data Preparation and Evaluation

4.2.1 Water Level Measurements

A monitoring network of piezometers and stilling wells, equipped with data loggers (Odyssey and Mini Diver) was installed along the lower reach of Stoney Creek to monitor the temporal and spatial variations of groundwater and surface water levels from 2015 to 2017. This network includes six cross sections where both groundwater and surface water levels were measured (Figure 2). Each cross section includes three piezometers, one on each bank and one within the stream channel, to measure piezometric head in the subsurface, and one stilling well to measure surface water level (stage) in the creek. All water levels were recorded at 10 minutes intervals. The cross-section locations were chosen to provide broad coverage of different features of Stoney Creek, including the headwaters at the outlet of Tachick Lake and various types of landscapes that Stoney Creek passes through. Groundwater levels were also measured manually with a water-level tape for calibration purposes. Details of the Stoney Creek monitoring network are described in the project report by Aghbelagh et al. (2018).

4.2.2 Climatic and Meteorological Conditions

Climate at the Vanderhoof meteorological station (the closest station to the SCW) is classified as cold and temperate. According to Köppen and Geiger (Beck et al., 2018), this climate is classified as Dfb, which refers to warm-summer humid continental climate. Based on the meteorological data recorded at the Vanderhoof station, the long-term (1991–2021) average annual temperature is 4.0 °C and the average annual precipitation is 554 mm (Table 4). Figure 3 shows precipitation data during the modelling period from 2015 to 2017. Based on comparison to the long-term average precipitation data, the year 2015 is classified as a normal year, 2016 as a wet year, and 2017 as a dry year.

4.2.3 Topography and Project DEMs

Topography in the SCW was represented by a 15-m resolution DEM provided by GeoBC (Figure 4a). Based on this DEM, ground elevation in the SCW ranges between 633 m above mean sea level (amsl) in the flat lowland areas up to a maximum of 1451 m amsl at the top of the watershed. Most of the watershed is within the lowland area. Topography within the modelling domain was derived from a 1-m DEM provided by LidarBC (Figure 4b). Use of this higher-resolution DEM within the modelling domain affords greater model accuracy of flows near Stoney Creek.

Table 4. Long-term (1991–2021) average precipitation (mm) and temperature (°C) recorded at the Vanderhoof station.

Variables	Jan	Feb	Mar	Apr	May	Jun	Jul	Aug	Sep	Oct	Nov	Dec	Average
Average Temperature (°C)	-8.1	-6.9	-2	3.7	9.9	14	16	16	11	4	-2	-7.6	4.0
Minimum Temperature (°C)	-11.4	-11	-7	-1	4	8.4	11	11	6.5	1	-5	-10.6	-0.3
Maximum Temperature (°C)	-3.5	-1.2	3.7	9.9	16	20	22	22	17	9	1.5	-3.7	9.4
Precipitation (mm)	46	29	34	37	45	57	49	42	46	65	60	44	554.0

Data source: climate-data.org and https://services.pacificclimate.org/met-data-portal-pcds/app/ (accessed Nov 2024)
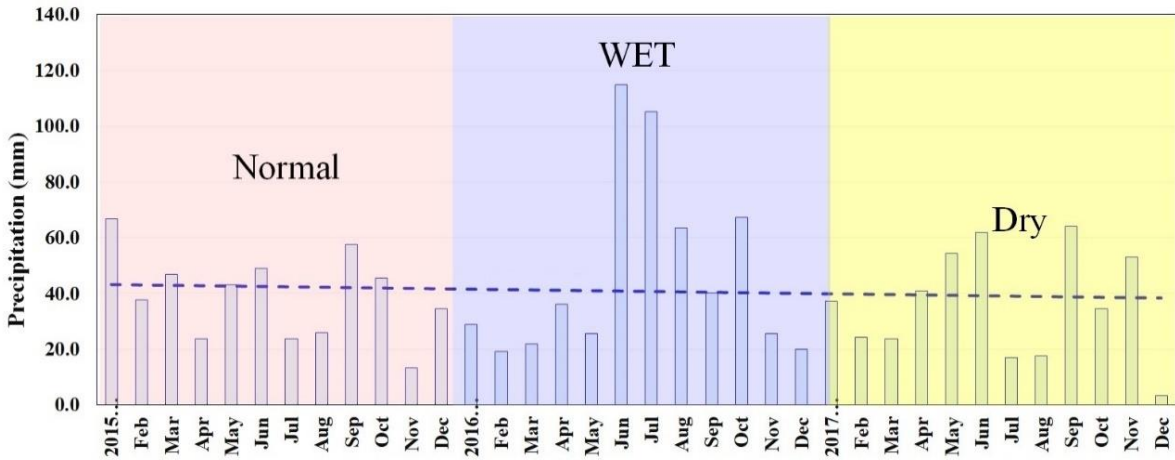
Figure 3. Monthly precipitation (mm) during the modelling period from 2015 to 2017.
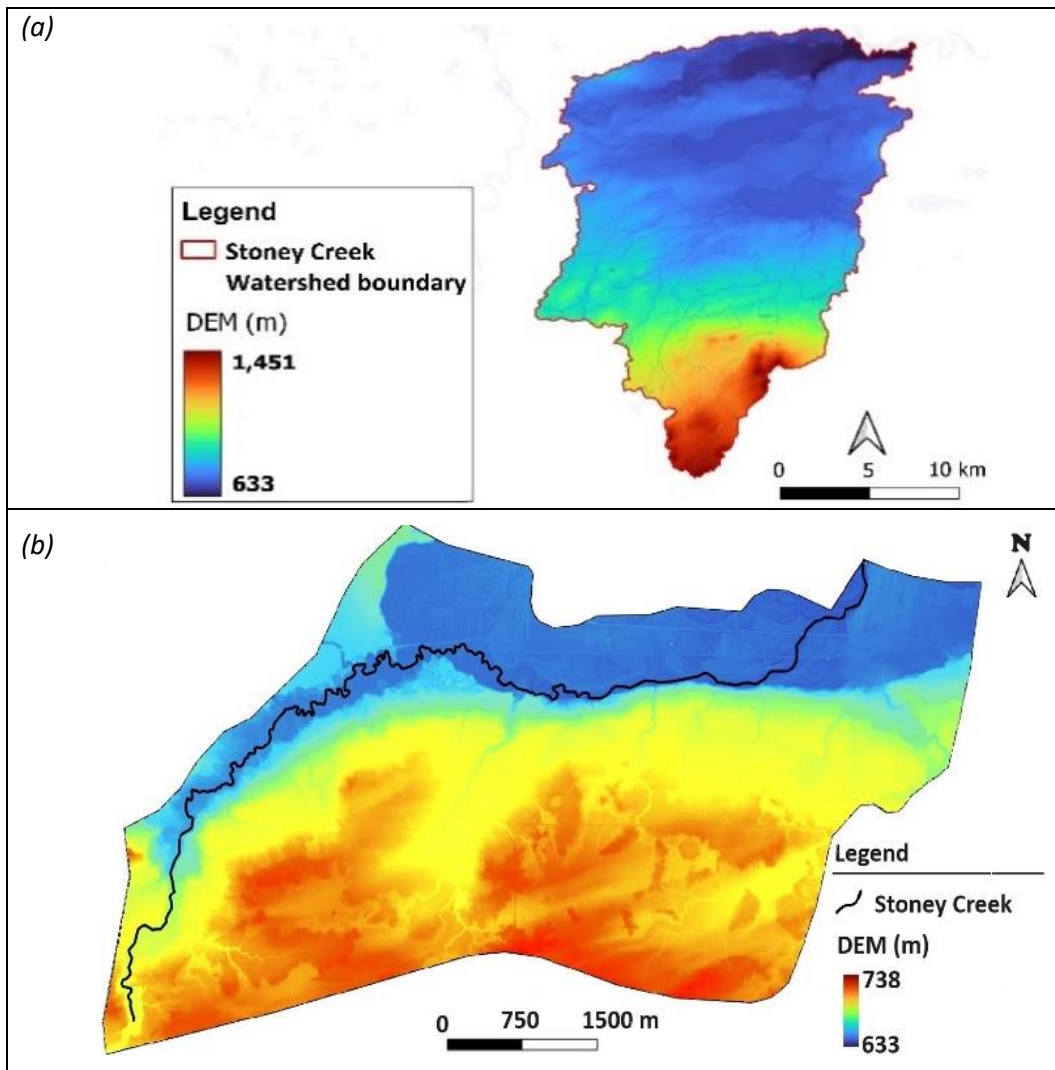
Figure 4. Project Digital Elevation Models: (a) a 15-m DEM map of the Stoney Creek watershed, and (b) a 1-m DEM map of the modelling domain (Source: GeoBC and LidarBC, respectively).

4.2.4 Land Use and Land Cover

Land use maps (Figure 5) for the SCW and modelling domain were developed from Sentinel-2 satellite data at 10 m resolution for the year 2022. Land use classification was a main consideration for estimating recharge rates from precipitation and calibrating the infiltration coefficients in the numerical model. Based on the land use map, 36% of the SCW area is covered by trees, 43% by crops, 3% by water, 10% by rangeland, and the remaining 8% consists of built areas. In addition, a time series analysis of land use change in the SCW indicates a 34% increase in 'built area' from 2017 to 2022. This increase in 'built area' implies that the study area has the potential for population growth and an increase in demand from groundwater resources in the future.

(a)

(b)
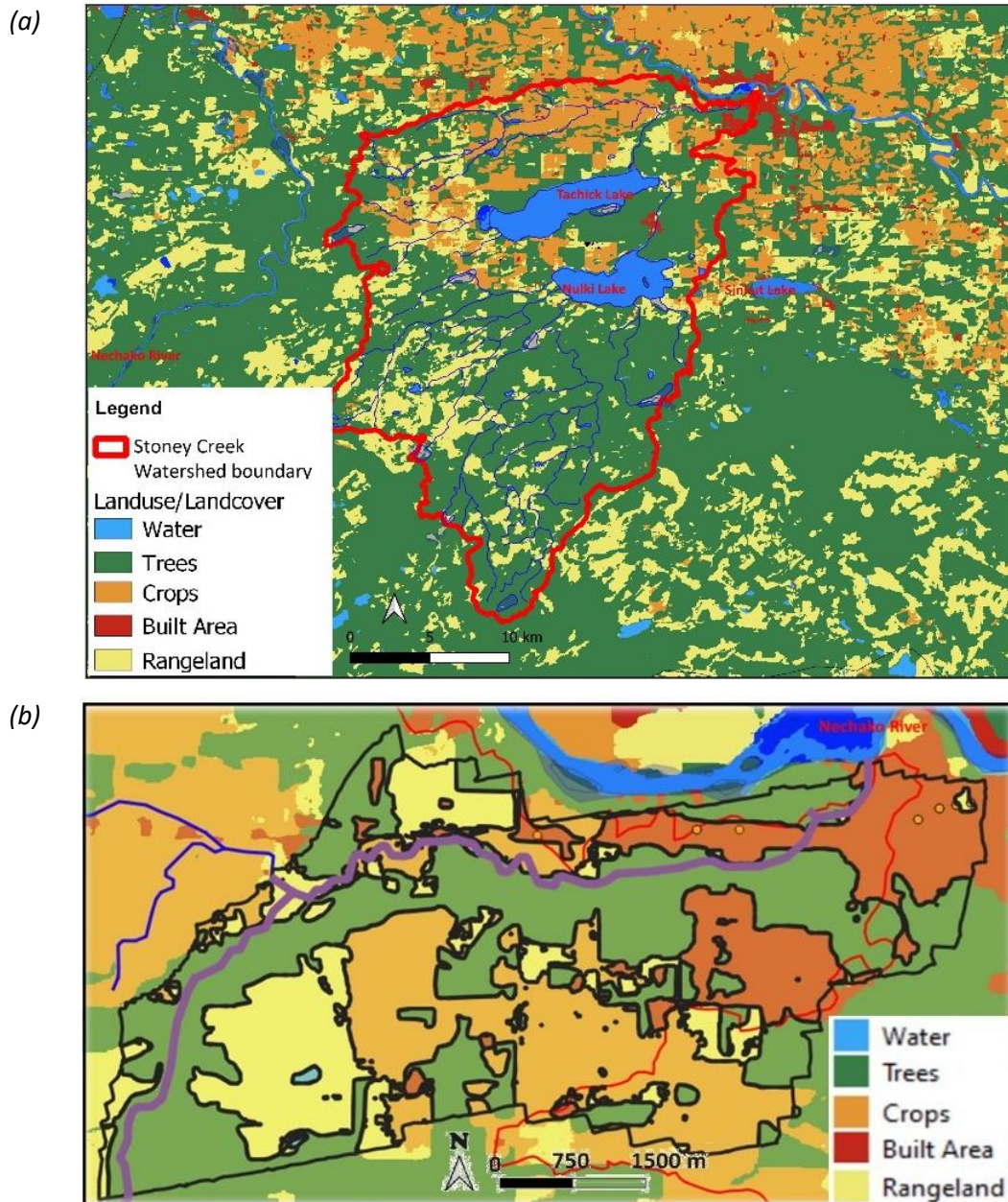
Figure 5. Land use and land cover maps for: (a) the Stoney Creek Watershed, and (b) the modelling domain.

4.2.5 Hydrogeologic Units

Figure 6 illustrates a schematic representation of the hydrogeologic units within the study area. The lowest unit is the bedrock (Figure 6 - Unit A), which was formed during the Jurassic Period through the accretion and fusion of the Intermontane Islands with the ancient North American continental edge. This process was accompanied by widespread faulting and fracturing of the bedrock. Above the bedrock, the lowermost layers consist of paleo-valley sands and gravels that date back to the pre-Fraser Glaciation (Figure 6 - Unit B). These sediments typically have limited areal extents and are not anticipated to develop into large, regionally extensive aquifers, primarily due to significant erosion that occurred after their deposition. However, they might be hydraulically connected to younger permeable sediments, potentially creating stacked aquifer systems, provided that the overlying fine-grained sediments (e.g., Figure 6 - Unit C) do not obstruct hydraulic continuity. The glaciofluvial sands and gravels deposited during the Fraser Glaciation (Figure 6 - Unit D) are expected to constitute regionally extensive aquifers. In addition, the overlying ice-advance glaciolacustrine sediments (Figure 6 - Unit E2), tills (Figure 6 - Unit F), and the glaciolacustrine sediments from the late Fraser Glaciation ice retreat (Figure 6 - Unit G) are generally characterized by fine grain size (Hinnell et al., 2020).
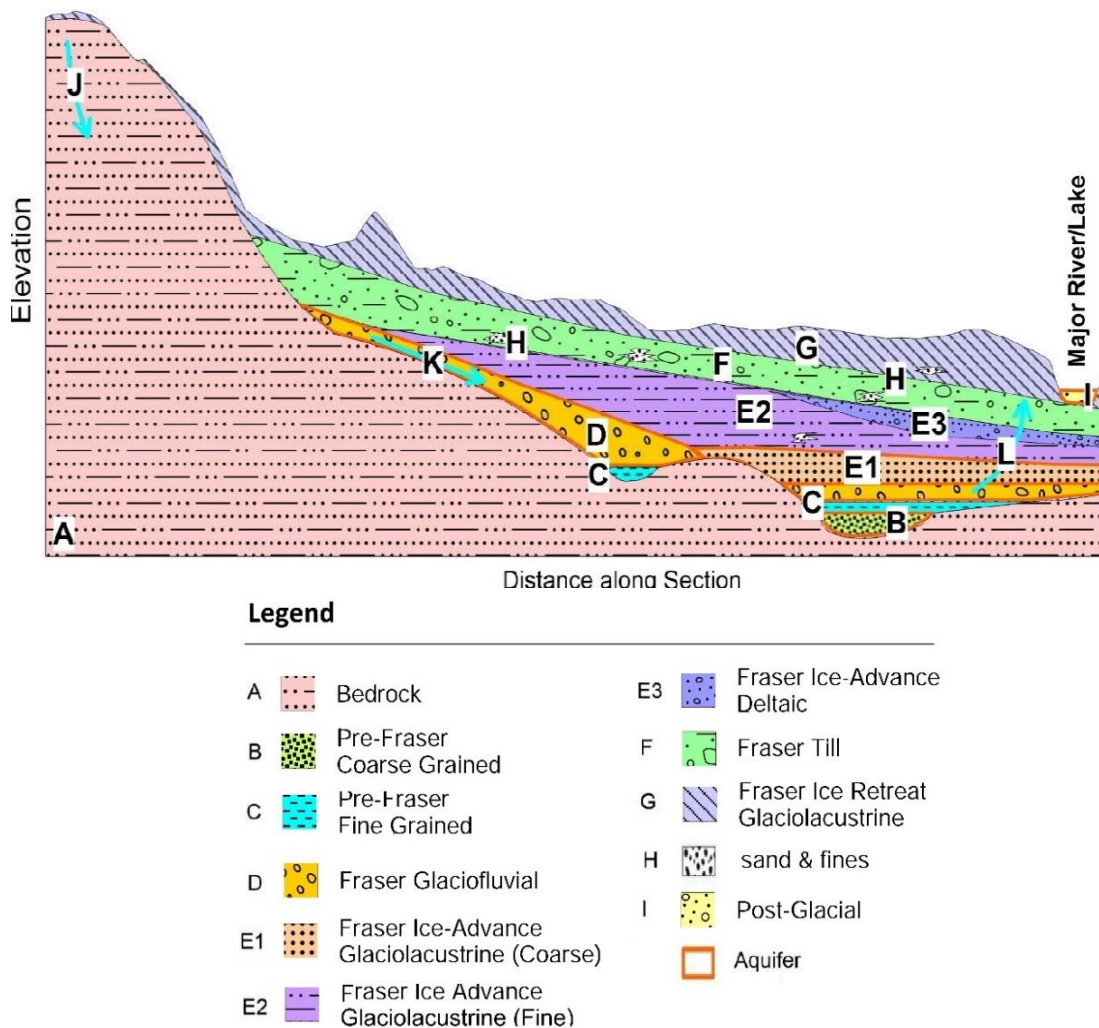
Figure 6. Schematic of hydrogeologic units of the study area (modified from Hinnell et al., 2020).

Generally, there are three major hydrogeologic units in the SCW that can be considered as water bearing: bedrock aquifers (Figure 6 - Unit A), confined aquifers (Figure 6- Unit D) and unconfined aquifers (Figure 6- Unit I). Bedrock is the lowest of the hydrogeology units. As the bedrock has been faulted and fractured, secondary permeability is expected in all types of bedrock. Further details of the aquifer characteristics are presented in Hinnell et al. (2020). Details of the regional geologic setting and aquifer characteristics of the Vanderhoof area are described in previous studies by Hinnell et al. (2020), Angen et al. (2018), Bordet et al. (2013), Clague (1981, 1988, and 2000), Clague et al. (1989), Cui et al. (2017), Ferbey (2011), Geoscience BC (2009), Sacco et al. (2017), Struik et al. (2007), Stumpf (2008), Stumpf et al. (2004), and Weatherup and Struik (1996).

5. METHODOLOGY

The GSI modelling framework for this study is shown in Figure 7. In this framework, a conceptual model of groundwater flow and GSI in the SCW was initially developed (step 2) based on the collection and evaluation of available data and information in the study area (step 1). The conceptual model forms the basis for design and development of the numerical model, which was constructed using the MODFLOW-USG code (step 3). The resulting numerical model is a three-dimensional (3-D) transient groundwater flow model. The model was calibrated with the available groundwater level monitoring data and surface water level data from Stoney Creek (step 4).
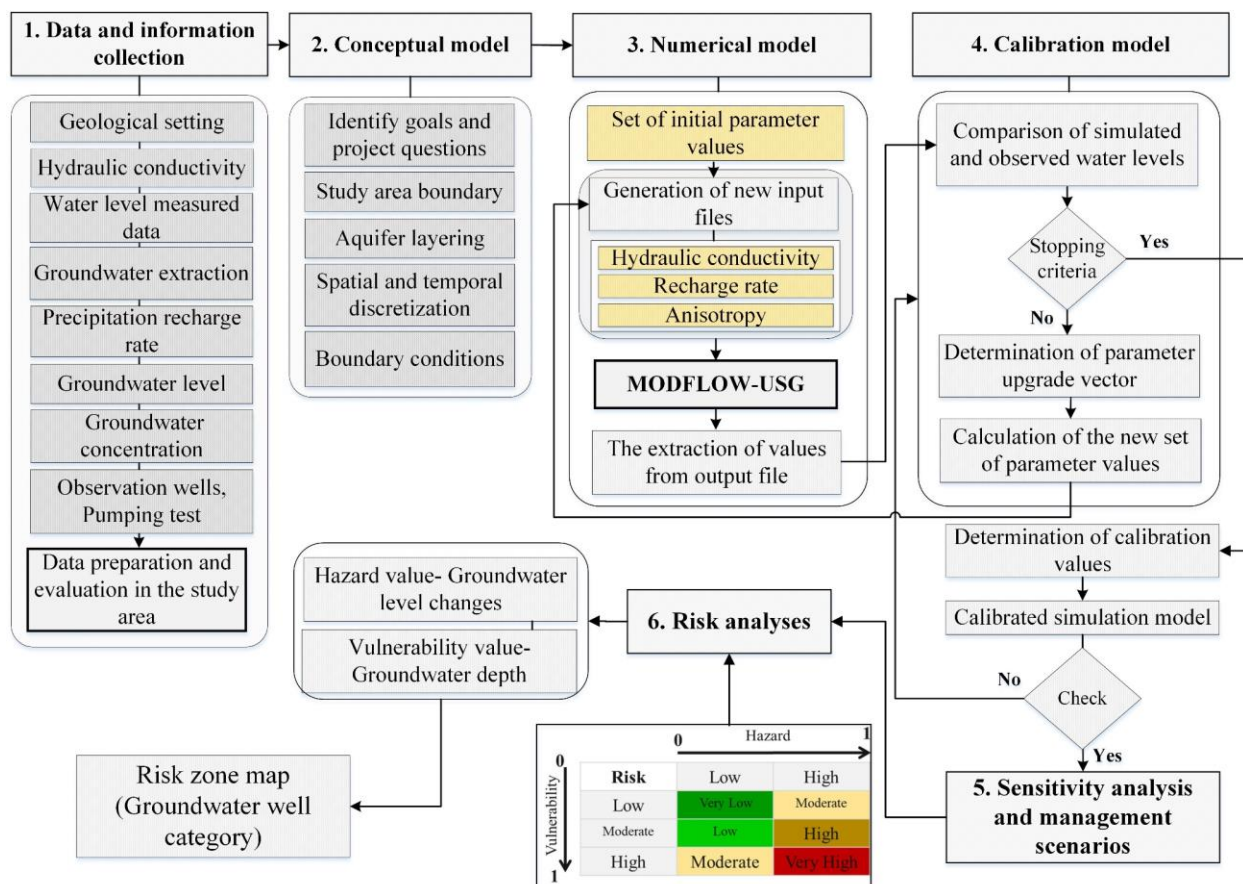
Figure 7. The groundwater and surface water interaction modelling framework.

The calibrated model was used to firstly assess the influence of selected model parameters on model predictions through a systematic sensitivity analysis, and secondly to simulate alternative management scenarios to investigate the impacts of various groundwater withdrawal scenarios on groundwater and Stoney Creek interaction (step 5).

In the final step, risk analysis was conducted to spatially quantify hazard and vulnerability from groundwater withdrawal through simulated water level changes from alternative well locations and aquifer materials (step 6). A risk zone map was prepared that spatially shows the relative risk of potential surface water level depletion from groundwater withdrawal in the SCW. Details of the modelling framework are provided in the following sub-sections.

5.1   Model Construction

5.1.1 Conceptual Model of Groundwater and Surface Water Interaction

Figure 8 illustrates the conceptual model of groundwater flow and interaction with Stoney Creek. The processes controlling the movement of water between atmospheric moisture, surface water and groundwater are spatially and temporally dynamic, and are difficult to observe and characterize. As shown in Figure 8, the interaction components include recharge from the river to the aquifer (Isw), and groundwater drainage (Dg) from the aquifer to the river. Both can be affected by precipitation, evaporation, and recharge from precipitation, as well as the river and aquifer characteristics such as river morphology, and homogeneity or heterogeneity of aquifer material (Mahmoodzadeh et al., 2024; Zhou et al., 2023).

The developed conceptual model forms the basis for construction of the numerical model including: selection of the numerical simulation approach and simulation model, stratigraphy modelling to identify representative geologic units, spatial and temporal discretization (grid construction), assignment of boundary conditions, model calibration, and identification of hydrogeologic parameters. Each of these model elements are detailed further in Sections 5.1.2 to 5.1.8.

W: Width of stream; L: length of stream; C:hydraulic conductance of the stream-aquifer interconnection; m: Thickness of streambed
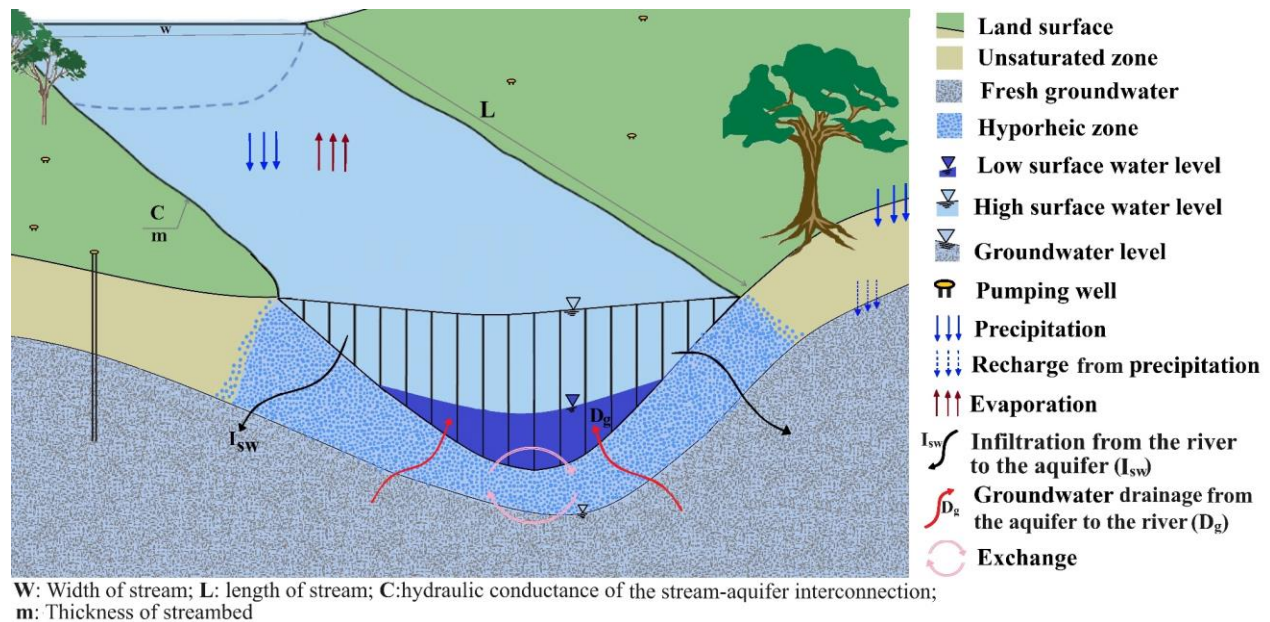
Figure 8. Conceptual model of groundwater and stream interaction at the reach scale.

5.1.2 Numerical Simulation Approach and Model Selection

A 3-D groundwater model was developed using the MODFLOW-USG code by the United States Geological Survey (USGS) (McDonald and Harbaugh, 1988). This code was selected because it is an established and widely used model for simulating groundwater flow and interaction with surface water using the finite difference solution method. Additionally, the model allows for use of an unstructured grid, providing flexibility in grid design that was used to focus resolution along Stoney Creek.

The model is based on Darcy's Law and the equation of mass conservation, resulting in a partial differential equation for groundwater flow, as given by Fetter (2001):

$$\frac{\partial}{\partial x}\left(K_x \frac{\partial h}{\partial x}\right) + \frac{\partial}{\partial y}\left(K_y \frac{\partial h}{\partial y}\right) + \frac{\partial}{\partial z}\left(K_z \frac{\partial h}{\partial z}\right) - W = S_s \frac{\partial h}{\partial t} \qquad \text{Eq.1}$$

where h is the groundwater water level (groundwater head) [L]; K_x, K_y, and K_z are the values of the hydraulic conductivity along the x, y, and z coordinate axes, which are assumed to be parallel to the major axes of hydraulic conductivity [L/T]; W represents the sources and/or sinks of water [1/T], S_s is the specific storage of the porous material [1/L]; and t is time [T].

Recharge from Stoney Creek to the aquifer and groundwater drainage from the aquifer to the creek were simulated based on Eq.2 in the numerical model (Harbaugh, 2005).

$$\begin{aligned} I_{sw} &= C \times \Delta h &&\text{if } \Delta h < 0 \\ D_g &= C \times \Delta h &&\text{if } \Delta h > 0 \end{aligned} \qquad \text{where} \quad C = \frac{K}{m} \times w \times L \qquad \text{Eq.2}$$

where I_{sw} is recharge from surface water [L³/T], D_g is groundwater drainage [L³/T], Δh is the difference in the head of aquifer and stream [L], L is the length of reach [L], C is the hydraulic conductance of the stream-aquifer interconnection [L²/T], K is the hydraulic conductivity of the streambed material [L/T], m is the thickness of streambed [L], and w is the width of the stream [L].

5.1.3 Stratigraphy Modelling

Lithology data from the existing well records (GWELLS) were used to construct the geology of the modelling domain. The lithology data were standardized using key lithology terms (e.g., gravel, sand and gravel, sand, silt, clay, sandstone, limestone, granite) to support subsurface interpretation. The stratigraphy characterization was determined with a focus on physical and hydraulic boundaries where possible (e.g., groundwater divides, geologic contacts, hydraulic boundaries, and surface water bodies). The 3-D stratigraphic model of the aquifer system was developed using an interpolation method (nearest neighbor and inverse distance weighting) with a base-to-top modelling sequence to develop the basement-topography map similar to the approach adopted by Karamouz et al. (2020). The map represents the local-scale elevation variations, both above and below ground, across the modelling domain.

The vertical lithology and stratigraphy modelling based on standardized lithology data are shown in Figure 9. Stratigraphy modelling in the Vanderhoof area, and a comparison between the model and the previously developed conceptual model is shown in Figure 9a. Figure 9b illustrates the stratigraphy modelling and vertical lithology in the modelling domain. The numerical model consists of eight distinct geologic layers, including three aquifer layers: 1) an unconfined surficial sand and gravel aquifer of post-glacial origin; 2) a confined glacial alluvial/glacial fluvial sand and gravel aquifer; and 3) a fractured bedrock aquifer.

(a)
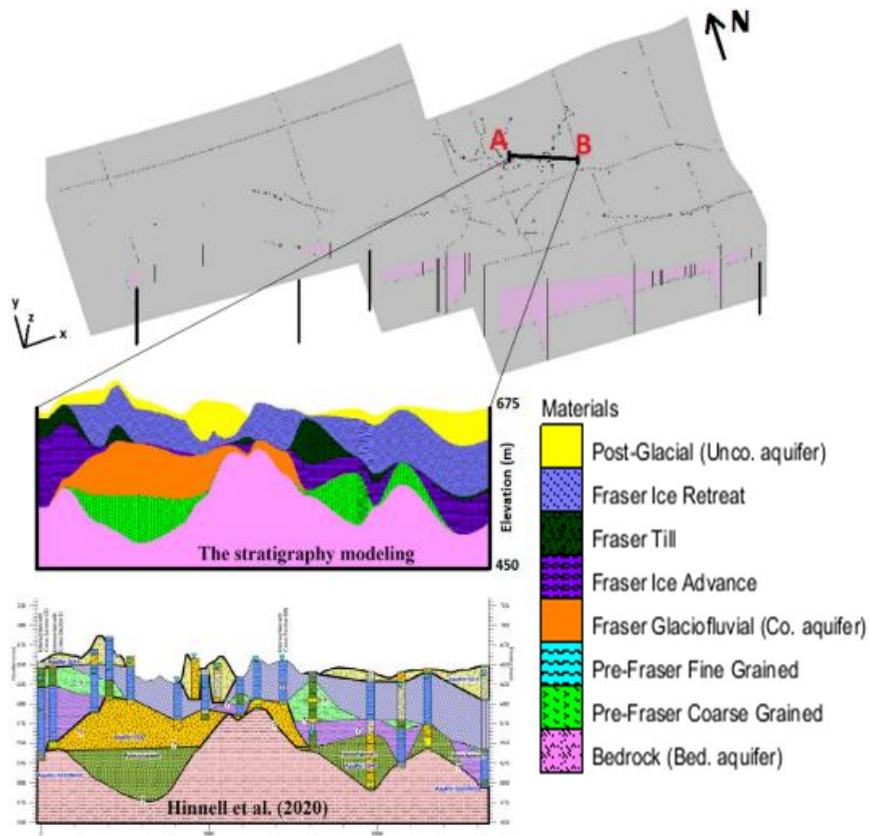
(b)
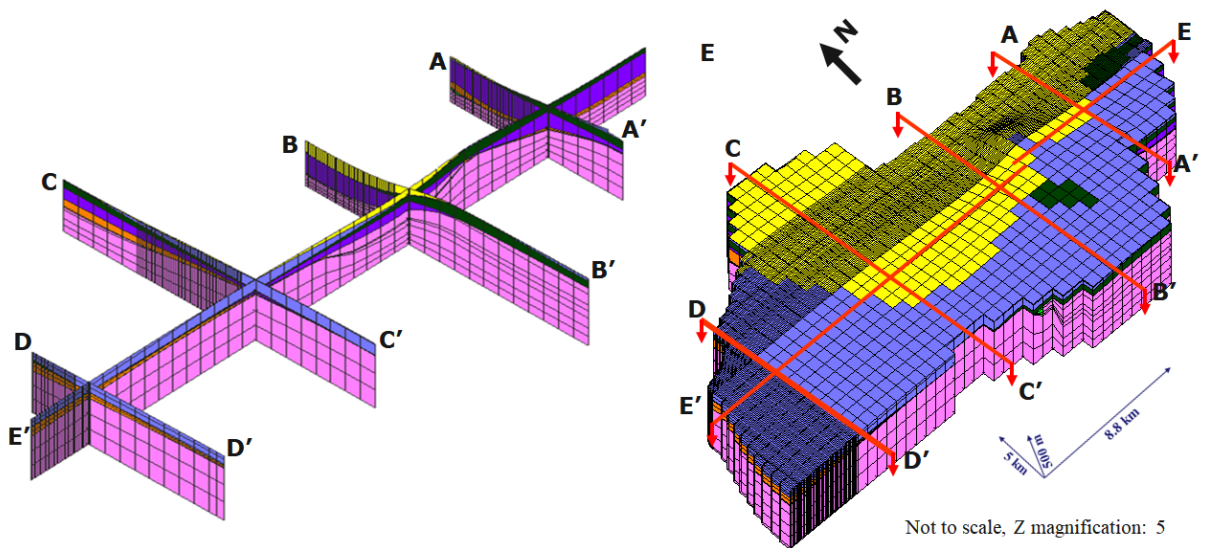
Figure 9. Illustration of the stratigraphy modelling showing: (a) results in the Vanderhoof area and comparison to a geologic cross-section from Hinnell et al. (2020), and (b) results in the modelling domain.

5.1.4 Boundary Conditions, Groundwater Recharge, and Withdrawal

The boundary conditions of the model were defined either as a specified head or no-flow. A plan view of the modelling domain and the assigned boundary conditions is illustrated in Figure 10. The north and south boundaries were assigned constant-head conditions based on groundwater-level contour lines derived from static water level data in GWELLS and groundwater level measurements at the project field site cross-sections. Note that due to the lack of time-dependent groundwater level data at the boundaries, a constant value is used for each month in the transient model. This means that the assigned groundwater level at the boundary remains constant for one time step in the transient model. No-flow boundary conditions were assumed along boundaries perpendicular to the groundwater flow paths on the west and northeast sides of the model domain. Stoney Creek was modelled with a specified head boundary where the head varies linearly along the stream.

Groundwater recharge from precipitation was modelled as direct infiltration from precipitation across the top layer of the model domain. In the study area, infiltration coefficients were initially estimated as a percentage of precipitation based on different land use and land cover (10–35%). Initial values for the different land use classes in the study area were selected based on typical infiltration coefficients from textbooks, such as Chow et al. (1988).
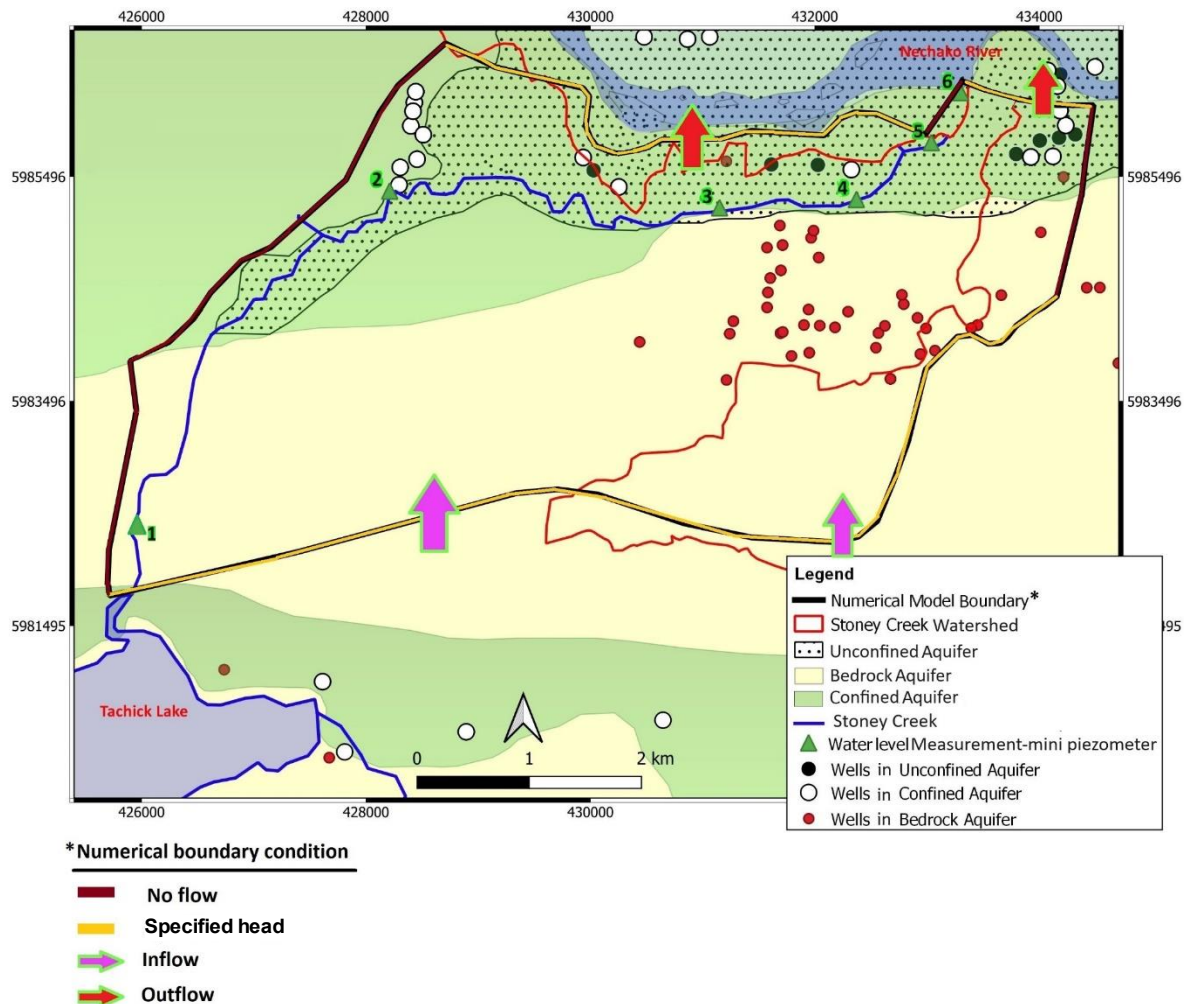
Figure 10. A plan view of the modelling domain with assigned boundary conditions.

Groundwater withdrawal, especially cumulative withdrawal, is one of the major factors that can influence both groundwater and surface water systems and their interactions. Figure 11a shows the location of all the groundwater wells in the Vanderhoof area. Groundwater withdrawal for a prolonged time not only lowers the water table immediately surrounding the wells but also leads to a drop in the regional water table and reduction of groundwater flow to nearby surface water bodies. Figure 11b shows the well locations in the modelling domain. Based on information in Forstner et al. (2018) and data available from iMapBC, the estimated volume of groundwater withdrawal[1] in the Vanderhoof area is 4600 m³/day, of which 110 m³/day occurs within the modelling domain respectively. Table 5 summarizes the volume of groundwater withdrawal, along with the consumption purposes in the Vanderhoof area and the modelling domain.

(a)

(b)
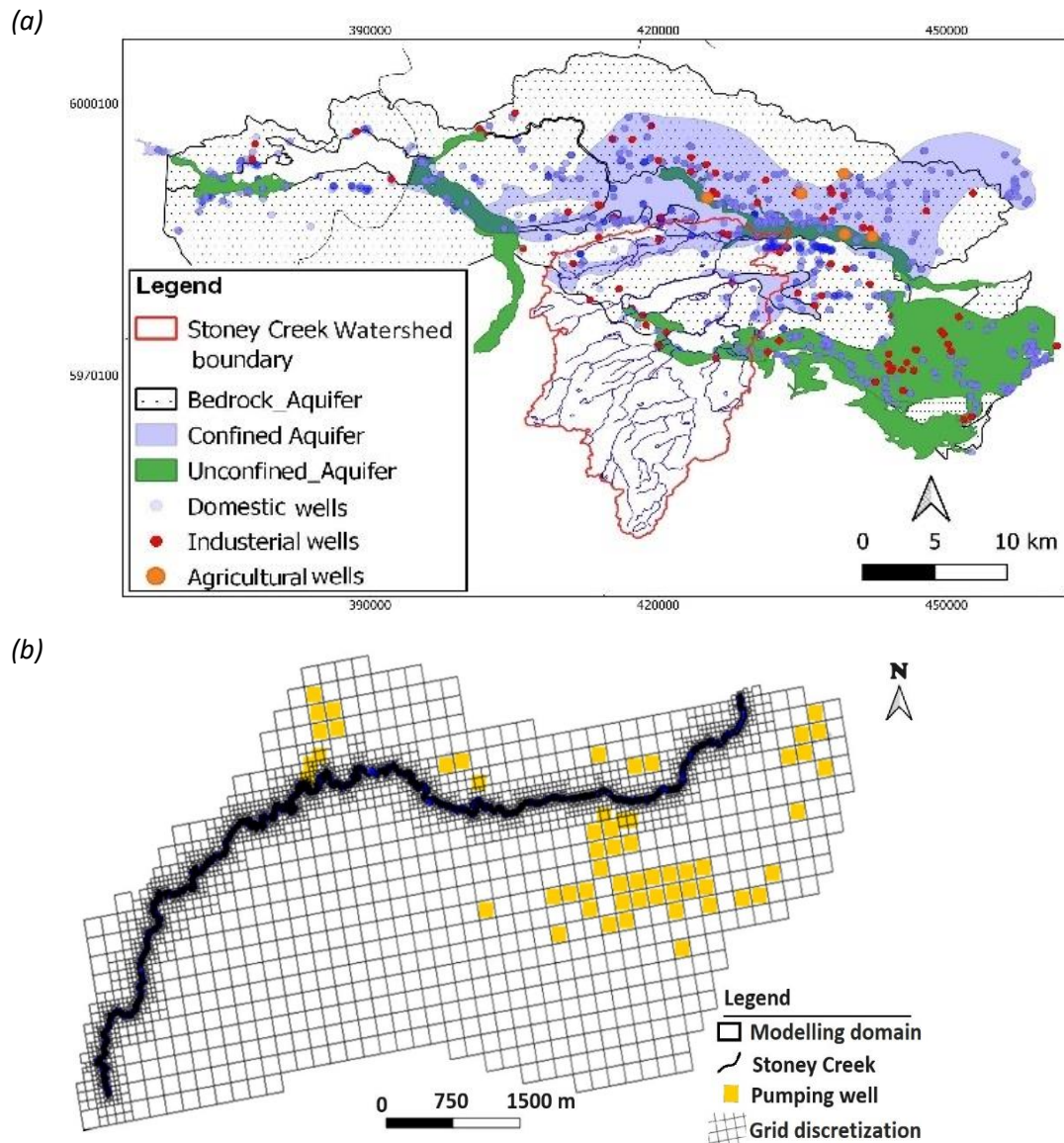
Figure 11. Location of groundwater wells in different types of aquifers including, unconfined, confined (unconsolidated), and fractured bedrock in the (a) Vanderhoof area, and (b) the modelling domain.

[1] Data source: https://apps.nrs.gov.bc.ca/gwells/aquifers

Table 5. Volume of groundwater withdrawal and consumption purposes (Source: Forstner et al., 2018, and iMapBC).

Aquifer Type	No. licenses	No. wells		Volume of withdrawal		Consumption purposes
		Vanderhoof area	Modelling domain	Vanderhoof *(m³/d)	Modelling domain (m³/d)	
Unconfined aquifer	31	256	7	1819.1	37.5	Domestic and industrial
Confined aquifers (confined and bedrock)	102	9919	48	2752.6	72.6	Mostly used for domestic
Sum	133	1170	61	4571.7	110.1	-

* It includes both licensed and unlicensed wells, with an assumed water use of 2 m³/day for the unlicensed wells.

5.1.5 Spatial and Temporal Discretization

To accurately model the flow dynamics of groundwater discharge to streams near the creek, a high-resolution DEM (i.e., 1-meter resolution) was used to obtain a more realistic representation of the stream network (i.e., more accurately reflect the elevation differences across the creek). Additionally, this approach provides the flexibility to select and refine the grid with sufficient resolution in the vicinity of the river. For the modelling domain, horizontal grid spacing ranged from a minimum of 3 m adjacent to the stream, up to a maximum of 200 m at the watershed boundaries (Figure 12).

Vertically, the model extends from the ground surface to a depth of 450 m above sea level. Vertical grid spacing ranges from 3 to 250 m to accommodate the different thicknesses of the geological units. The 3-D spatial discretization of the modeling domain is shown in Figure 12.
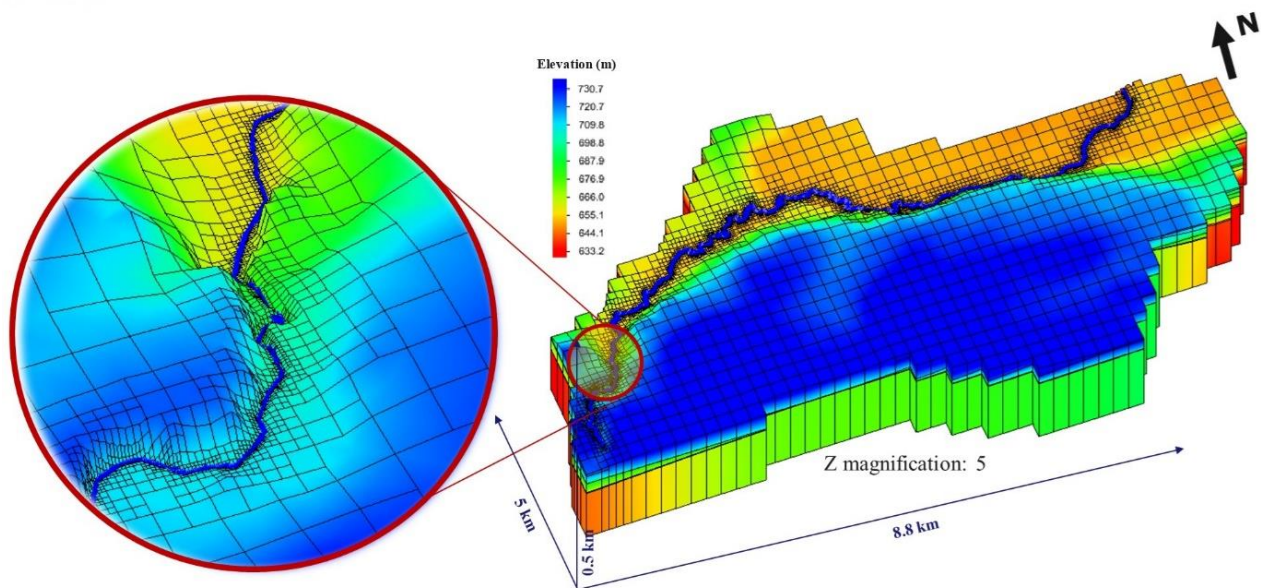
Figure 12. 3-D unstructured grid spatial discretization of modelling domain across Stoney Creek.

For the simulation model the total simulation period was three years, from 2015 to 2017. A total of 36-time steps were specified in the model, each representing a one-month period.

The simulation setup, model characteristics, and model control parameters are summarized in Table 6.

Table 6. Summary of simulation setup and model characteristics in the SCW.

Characteristics	Description
Simulation setup	
Modelling package	MODFLOW-USG (Harbaugh, 2005)
Porous media	Heterogeneous
Simulation mode	Steady-state and transient
Time step	1 month
Total transient simulation time	3 years (36-time steps)
Total active grid cells	120,575
Grid dimension (horizontal direction) (m)	3-200
Grid dimension (vertical direction) (m)	3-250
Model Characteristics	
Flow Package	Layer Property Flow (LPF)
Linear system solver	Sparse Matrix Solver (SMS)
Maximum number of outer iterations	500
Number of inner iterations	100
Nonlinear and linear solution method	Picard and PCGU
Head change criterion for convergence	0.0001
Residual criterion for convergence	0.0001

5.1.6 Model Calibration

In this study, model calibration was conducted using both automated procedures in the PEST code and trial-and-error methods. The calibration data for both the steady-state and transient model calibrations were: 1) groundwater and Stoney Creek water level measurements at the field site cross-sections from 2015 to 2017, and 2) static groundwater level data available from GWELLS in both unconfined and confined aquifers. We assumed that the long-term static groundwater level data was not influenced by pumping. The transient water level measurements at the field cross sections and the static water level data in the pumping wells were weighted equally during the calibration procedure.

Model calibration was achieved through a stepwise process. An initial calibration was conducted for aquifer hydraulic conductivities and anisotropy ratios of the aquifer model layers, and the riverbed hydraulic conductivity. The calibration for the aquifer hydraulic conductivity and anisotropy was done automatically using PEST, while the riverbed hydraulic conductivity was calibrated by trial-and-error.

Once calibrated values for anisotropy ratios, aquifer and riverbed hydraulic conductivity were obtained, these values were held constant. Next, the calibration of groundwater recharge from precipitation (infiltration coefficient) was carried out to ensure that the water levels observed in the measurement cross sections closely matched the simulated values. The calibration of the infiltration coefficient was performed by trial-and-error. Then, the infiltration coefficient values obtained from the steady-state model were used for the transient model along with the hydraulic conductivity values. Note that the

calibrated infiltration coefficients were applied to all time steps (36-time steps during 2015–2017) in the transient model.

Two main criteria were defined to establish convergence of the calibration process in PEST. In the first criterion, the calibration was considered complete once the difference in parameter values over two successive steps was less than the convergence limit over the maximum number of convergence iterations. The calibration was also considered complete if the maximum parameter difference during the maximum number of parameter change iterations is less than or equal to the parameter change criterion.

In the trial-and-error method, the calibration process was considered complete once the values of the root mean square of error (RMSE) and the mean absolute error (MAE) do not decrease further. The statistical parameters including the mean error (ME), mean absolute error (MAE), root mean square error (RMSE) and squared correlation coefficient (R^2) were used to evaluate the performance of the calibrated steady-state and transient models as stated in equations 3-5, respectively (Karamouz et al., 2020; Rajaeian et al., 2024).

$$MAE = \frac{\sum_{i=1}^{n}|S_i - O_i|}{n} \qquad \text{Eq.3}$$

$$RMSE = \sqrt{\frac{\sum_{i=1}^{n}(S_i - O_i)^2}{n}} \qquad \text{Eq.4}$$

$$R^2 = \frac{\sum_{i=1}^{n}(O_i - \bar{O})^2 - \sum_{i=1}^{n}(S_i - \bar{S})^2}{\sum_{i=1}^{n}(O_i - \bar{O})^2} \qquad \text{Eq.5}$$

where S_i is the ith value of the simulated groundwater level at the observation location, O_i is the ith value of the observed (measured) groundwater level, n is the total number of observation data, $\bar{O}$ and $\bar{S}$ are the mean of the observed and simulation groundwater level, respectively.

5.1.7 Hydrogeologic Parameters

The hydraulic conductivity of major aquifers in the study area (SCW) is expected to vary significantly from location to location. The hydraulic conductivity for confined and bedrock aquifers was initially determined from the results of two pumping tests conducted in provincial observation wells #516 and #455 near the study area (personal communication with WLRS). Well #516 is completed in a confined sand and gravel aquifer. Well #455 is completed across the interface of the bedrock and unconsolidated aquifers and therefore is assigned to the bedrock aquifer during this study (#517 is currently linked to the unconsolidated aquifer in GWELLS). For other geological model layers including the unconfined aquifer, the initial values of hydraulic conductivity were determined using textbook values (Fetter, 2001). The aquifer anisotropy is the ratio of vertical to horizontal hydraulic conductivity (K_v/K_h). The initial value of the anisotropy ratio was chosen at 0.1 and was adjusted to 0.2 during model calibration.

In this project, streambed thickness is assumed to be 1 m, and the width of Stoney Creek ranges from 3 to 8 m (measured on Google Earth map). Reported values for hydraulic conductivity of streambed sediments vary over a wide range (Strasser et al., 2015; Delleur, 2007); therefore, this parameter was determined through the calibration process. To this end, the riverbed hydraulic conductivity was initially set to a value of 0.2 m/d based on literature information (Fetter, 2001; Strasser et al., 2015; Stefania et al., 2018; Aghbelagh et al., 2018) and was adjusted to 0.5 m/d during model calibration.

Table 7 shows the initial and calibrated values of hydrogeologic model parameters. Additionally, Table 7 shows model values for storage parameters including porosity and specific yield, which account for storage capacity and moisture retention in the unconfined aquifers, and specific storage, which accounts for storage capacity in the confined aquifers. The model values for the storage parameters were not determined by model calibration but rather were specified based on information from previous studies (e.g., Aghbelagh et al., 2018) and published textbook values (e.g., Freeze and Cherry 1979; Fetter, 2001).

Groundwater recharge from precipitation (infiltration coefficient %) was modelled as direct infiltration from precipitation across the top layer of the model domain. Initial values of infiltration coefficients were refined during model calibration, with calibrated values summarized in Table 8. These calibrated infiltration coefficients are in a similar range to values reported by Forstner et al. (2018), who calculated infiltration rates of 32% of precipitation based on the aquifer-scale HELP method and 33% of precipitation for the global hydrologic model in B.C.

Table 7. Initial and calibrated values of hydrogeologic parameters in the numerical model.

Parameters (material)*	Unit	Range	Initial value	Calibrated value
Hydraulic conductivity – unconfined aquifer (G, SF, SG, S)	(m/d)	10 to 25	10	11
Clay and silt		0.001 to 0.3	0.001	0.2
Till		0.01 to 0.2	0.1	0.1
Clay and silt		0.0008 to 0.002	0.0009	0.0017
Hydraulic conductivity - Confined aquifer (S, SF, and SG)		15 to 25	20	22
Clay		0.0001 to 0.005	0.0001	0.0002
Hydraulic conductivity – confined aquifer (SF, G, and S)		1 to 25	15	20
Hydraulic conductivity – bedrock aquifer		0.1 to 0.9	0.4	0.9
($K_{vertical}$/$K_{horizontal}$) (Anisotropy ratio)	-	0.1 to 0.3	0.1	0.2
Riverbed hydraulic conductivity	(m/d)	0.2 to 0.5	0.2	0.5
Specific yield	-	-	0.3	Not calibrated
Specific storage	(1/m)	-	0.00005	
Porosity	-	-	0.3	

*G: gravel, SF: sand and fines, SG: sand and gravel, S: sand

Table 8. Calibrated infiltration coefficient (% of precipitation) in the modelling domain.

Land use/cover	Range	Initial value	Calibrated value
Water	25-70	25	30
Trees	25-50	30	33
Crops	30-60	40	35
Built area	5-10	10	9.5
Rangeland	20-50	20	27

5.2 Sensitivity Analysis

Sensitivity analysis is a crucial part of the numerical model because of the uncertainty in the key parameters. For example, in this study, the same hydraulic conductivity was assigned to each geological layer, and a uniform riverbed hydraulic conductivity was applied along the entire length of Stony Creek. Therefore, a sensitivity analysis is required to evaluate the related uncertainties. The numerical model parameters, such as the hydraulic conductivity of unconfined and confined aquifers, as well as the infiltration coefficients, were selected for sensitivity analysis. The hydraulic conductivity of bedrock aquifers was not selected for sensitivity analysis because it is expected that the hydraulic connection between bedrock aquifers and Stoney Creek is negligible.

The sensitivity analysis provides an assessment of the influence of model parameters on model predictions of hydrogeological processes, such as the volume of aquifer recharge from infiltration of streamflow in Stoney Creek (I_{sw}). By comparing the relative effect of changes in model parameters on model predictions, the most sensitive parameters of the simulated system are identified, which can then help to focus calibration and data collection efforts. In this sensitivity analysis, the numerical model parameters (see Table 9) were varied within a reasonable range (e.g., from -25% to +25%), similar to the approach adopted by Yihdego and Becht (2013) and Ketabchi et al. (2024). This range effectively captured the parameter variability and reflects the sensitivity of the model predictions from these changes. The parameter values in Table 9 are evaluated in the sensitivity analysis process and the results are discussed in Section 6.3.

Table 9. Parameters selected for sensitivity analysis in the GSI numerical model of the SCW.

Parameters	Description	Reference
Hydraulic conductivity (K)_all	Hydraulic conductivity (K) in all main aquifers (Unconfined, Confined, and Bedrock) decreased (up to -25%) and increased (up to 25%).	Yihdego and Becht (2013); Mahmoodzadeh et al. (2014); Forstner et al. (2018); Ketabchi et al. (2024)
K_Con	K in the confined aquifer, decreased (up to -25%) and increased (up to 25%).	
K_Uncon	K in the unconfined aquifer, decreased (up to -25%) and increased (up to 25%).	
Riverbed hydraulic conductivity (K_b)	K_b decreased (up to -25%) and increased (up to 25%).	Strasser et al. (2015); Naganna et al. (2017); Ketabchi et al. (2024)
Infiltration coefficient (IC)	Infiltration coefficient (IC) decreased (up to -25%) and increased (up to 25%).	Becht (2013); Forstner et al. (2018); Ketabchi et al. (2024)

5.3 Defined Management Scenarios

In this study, ten management scenarios (MS1-MS10) were simulated with the numerical model to assess the impacts of various conditions on GSI. The scenarios include the decrease in groundwater levels at the southern (MS1) and northern (MS2) boundaries of the modelling domain to evaluate the effects of lower water tables due to cumulative groundwater withdrawal over time. Scenarios MS3 explores the implications of increased groundwater withdrawal by up to 50% within the modelling domain due to the future water demand.

Different climatic conditions are also considered, with MS4 and MS5 representing wet and normal conditions respectively, and MS6 focusing on dry conditions. Scenarios MS4 to MS6 were defined based

on the analysis of the precipitation data during the simulation period (2015 to 2017). In this analysis, three precipitation categories were defined as the normal (2015), wet (2016), and dry (2017) conditions for each year, based on the average precipitation. These three scenarios assume that the precipitation continues in the same pattern during the whole simulation period.

Scenarios MS7 through MS9 examine the effect of varying rates of groundwater withdrawal (e.g., 10% or 50% increases) during drought conditions (MS6) or with regional decreases in groundwater levels within the modelling domain. Lastly, scenario MS10 is defined by a 10% increase in groundwater withdrawal, combined with declines at both the southern and northern boundaries of the modelling domain, representing the worst-case scenario in this study. Table 10 describes the simulated management scenarios.

Table 10. Simulated management scenarios to assess the influence of regional groundwater levels, climatic, groundwater pumping levels on groundwater-surface water interaction in the SCW.

Name [a]	Abbreviation [b]	Description	Reference
MS1	Head-2m_Southern boundary	Groundwater level along the southern boundary of the study area is decreased by 2 m.	Yihdego and Becht (2013) Mahmoodzadeh et al. (2014) Forstner et al. (2018) Ketabchi et al. (2024)
MS2	Head-2m_Northern boundary	Groundwater level along the northern boundary of the study area is decreased by 2 m.	
MS3	GWP10,25,50%	Groundwater pumping from the unconfined aquifer is increased up to 50% in model domain due to increasing water demand in the future.	
MS4	WET condition	It is assumed that the study area is under wet conditions, i.e., above average precipitation (Based on the analysis of the precipitation).	
MS5	Normal condition	The study area is under normal precipitation conditions (Based on the analysis of the precipitation).	
MS6	DRY condition	The study area is under dry conditions, i.e., below average precipitation (Based on the analysis of the precipitation).	
MS7	DRY condition and GWP50%	The study area is under dry conditions and a 50% increase in groundwater pumping occurs.	
MS8	CGP1	It is assumed that a 10% increase in groundwater pumping and a decline in the groundwater level occurs at the northern boundary of the model.	
MS9	CGP2	10% increase in groundwater pumping and a decline in the groundwater level occurs at the southern boundary of the model.	
MS10	CGP3	10% increase in groundwater pumping and a decline in the groundwater level occurs at both the northern and southern boundaries of the model.	

[a] MS: management scenarios
[b] GWP: groundwater withdrawal; CGP: cumulative groundwater pumping

5.4 Risk Concept

Assessing the risk of streamflow depletion due to groundwater well pumping requires a comprehensive framework that incorporates the GSI model. The risk assessment analysis that is a part of this framework is based on the established methodologies employed in many previous studies with (e.g., De Stefano et al., 2017; Sanchez and Etebari, 2019; Karamouz et al., 2020).

The risk analysis is comprised of two main components: hazard and vulnerability. The hazard component addresses the potential events that could negatively impact streamflow, such as increased groundwater pumping, which is illustrated in this project through the water level changes map. Vulnerability evaluates how susceptible the groundwater and Stoney Creek systems are to these hazards. This includes analyzing the pumping well spatial distribution and depths of wells. In this study, the vulnerability of pumping wells was classified by assigning wells to various risk zones based on water level changes in the connected streams due to groundwater withdrawal (resulting from the numerical model), well location and depth, and aquifer type that the well is pumping from. Based on this concept, hazard and vulnerability are determined for each groundwater pumping well and a risk map is prepared. Pumping wells in the risk map are grouped into six relative risk categories as shown in Figure 13.

Figure 13. Risk components in six relative categories.

6. RESULTS AND DISCUSSION

In this section, the calibration of the numerical model is discussed. The groundwater level distributions in the modelling domain and the spatial distribution of GSI along Stoney Creek are described under current conditions (i.e., base scenario). In addition, the results of the sensitivity analysis and management scenarios are discussed, with a focus on the effects of groundwater withdrawal. Finally, the results of the risk analyses are presented to classify pumping wells and determine the risk zones based on changes in groundwater levels due to the pumping.

6.1 Model Calibration

The calibration of the steady-state and transient models was performed using static water level data measured in both confined and unconfined aquifers, as well as water levels measured in piezometers (18 locations in six cross sections) and stilling wells (five locations in five cross sections). As discussed in Section 5.1.6, the hydraulic conductivity of aquifers, streambed hydraulic conductivity, infiltration coefficients, and anisotropy ratios are the selected calibration parameters.

Results of the steady-state model calibration are shown in Figure 14. The mean absolute error (MAE) between the measured (observed) and simulated groundwater levels is 0.82 m and 0.96 m for the observed groundwater levels in piezometers and static groundwater levels in other wells, respectively.

Results of the steady-state model calibration were subsequently used as initial conditions in transient model simulations. Monthly groundwater level data measured in piezometers were used as the observed data in the unconfined aquifer for transient model calibration. In the transient model, the infiltration coefficients were also calibrated using the trial-and-error method.

Table 11 summarizes the calibration results for the steady-state and transient models. The errors obtained from the steady-state and transient simulations indicate good overall agreement between the observed and the simulated groundwater levels.

(a)   *(b)*
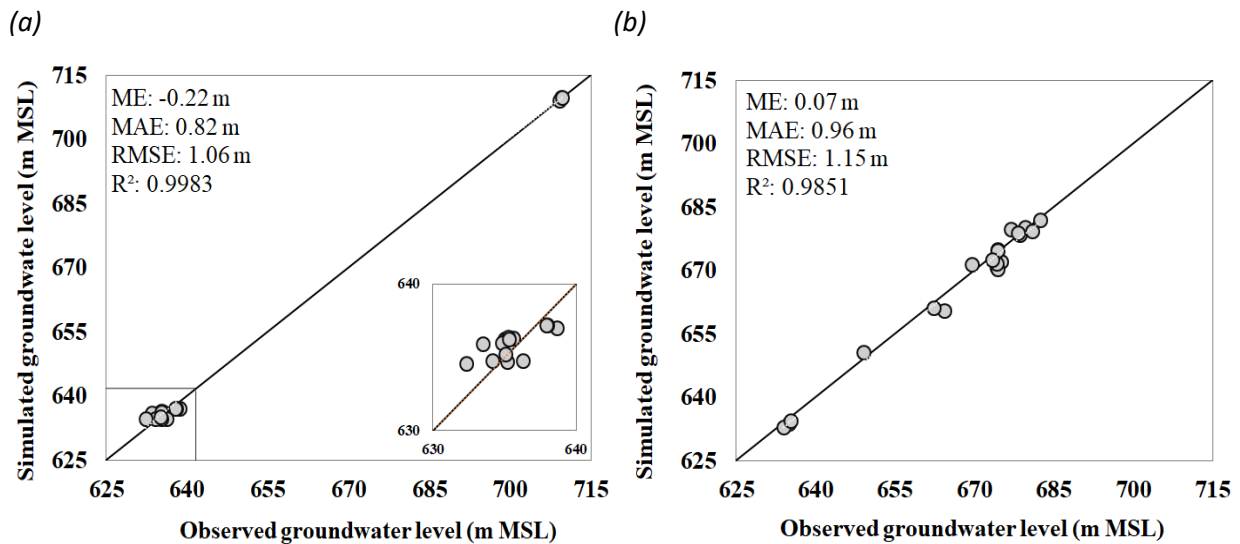
Figure 14. Comparison of observed and simulated groundwater levels from the steady-state model: (a) comparisons with groundwater levels measured in study area piezometers, and (b) comparisons with static groundwater level data from both unconfined and confined aquifer wells in GWELLS. Gray circles (◎) represents measured and simulated water levels in each piezometer and well.

Table 11. Statistical measures of steady-state and transient model calibration results.

Simulation model	Location of Measured groundwater levels	ME (m) [a]	MAE (m) [b]	RMSE (m) [a]	R² [d]
Steady-state	Piezometers	-0.22	0.82	1.06	0.9983
	Pumping wells	0.07	0.96	1.15	0.9851
Transient	Piezometers	-0.29	1.024	1.24	0.9959

[a] Mean error, [b] Mean absolute error, [c] Root mean square error (RMSE), [d] Squared correlation coefficient (R²)

6.2   Simulated Groundwater and Surface Water Interaction in the Study Area

Figure 15 illustrates the simulated spatial distribution of the groundwater levels in the steady-state model. This figure represents the overall regional groundwater levels; though they vary across different aquifers (i.e., unconfined, confined, and bedrock aquifers). It is worth mentioning that an unconfined layer was defined at the southern boundary based on the measurement cross sections. However, there are no regional unconfined aquifers extending across the southern part of the modelling domain. The overall groundwater levels in the south of the study area are 715 masl, decreasing gradually towards the north to 622 masl. Additionally, the direction of overall regional groundwater flow is downgradient (from south towards north) and perpendicular to the groundwater levels contours, but they have different flow patterns at different cross sections and represent local flow directions.

Figure 16 shows the simulated steady-state spatial distribution of groundwater-surface water interaction along Stoney Creek. In this figure the black circles indicate gaining reaches where groundwater discharge contributes to the flow in Stoney Creek (Dg). The pink circles indicate losing reaches where groundwater receives recharge from Stoney Creek (Isw). The simulation results show that groundwater discharge is a significant source of streamflow in Stoney Creek. Simulated volumes of groundwater discharge to Stoney Creek range between 0.01 to 23.6 million cubic meters (MCM/yr) depending on the location of the discharge. The length of the stream reach (segment) and the associated Dg and Isw ranges are shown in Table 12.
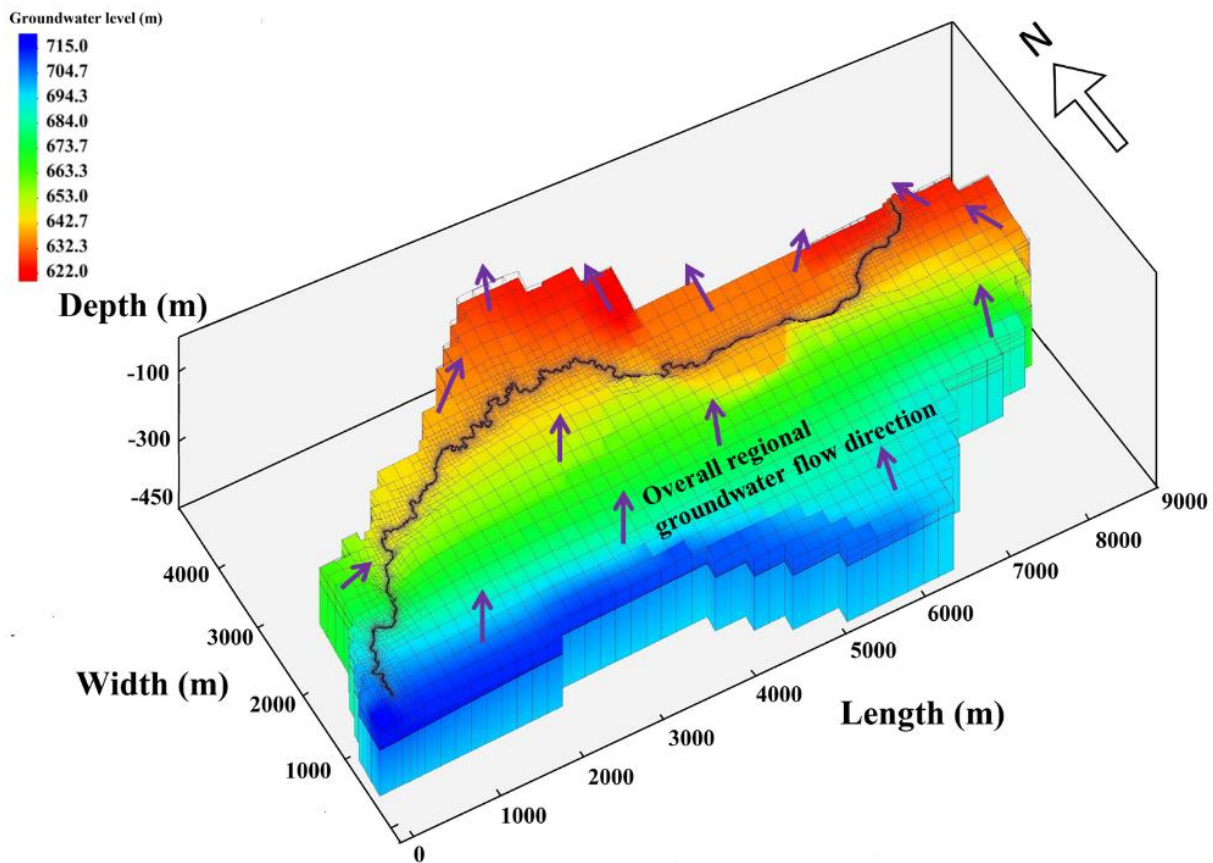

Figure 15. Simulated spatial distribution of the groundwater levels and the regional groundwater flow direction in the steady-state model.
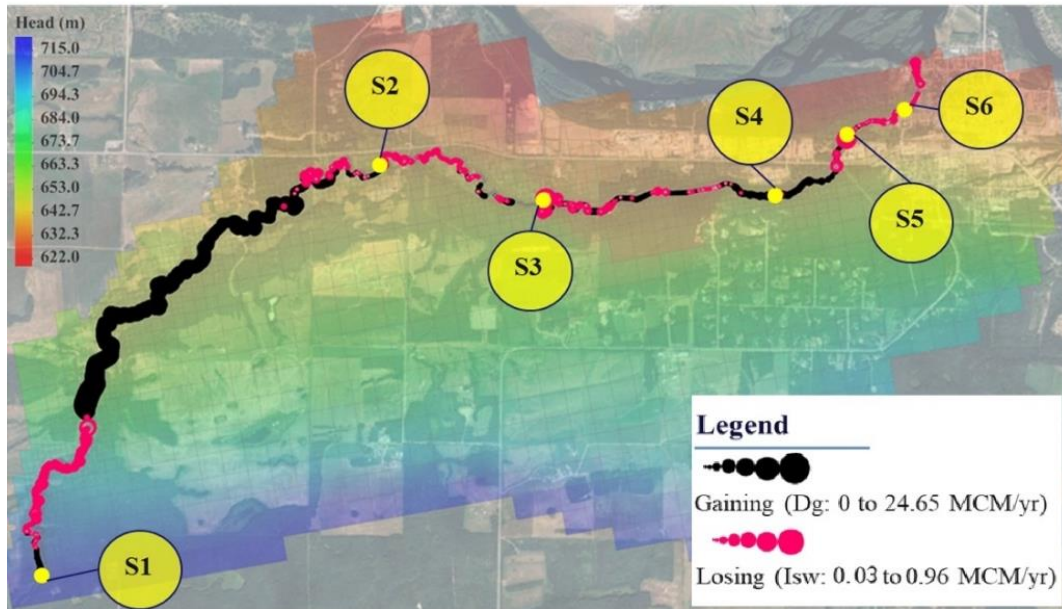
Figure 16. Steady-state simulation results showing the spatial distribution of groundwater and Stoney Creek interactions. Yellow circles (S1) show the locations of the measurement cross sections

Table 12. Steady-state model results for annual groundwater discharge to Stoney Creek (Dg) and annual recharge from Stoney Creek to groundwater (Isw). The location of stream reaches is shown in Figure 16.

Stream reach (Segment)	Length of the stream reach (km)	Discharge (MCM/yr)	
		Isw	Dg
1-2	7.8	0.66	23.66
2-3	3.0	0.06	0.39
3-4	1.4	0.03	0.46
4-5	0.8	0.11	0.13
5-6	0.6	0.05	0.01
6-end	0.3	0.05	-

Figure 17 depicts the simulated groundwater water levels for each cross section of Stoney Creek. Also, in this figure, the local groundwater flow direction was determined based on the simulated groundwater levels of the left bank, in-stream, and right bank. The measured data are the average water levels for three years (2015 to 2017), and the simulated results are extracted from the steady-state model. At cross section #1, the simulated groundwater levels on either bank are higher than the Stoney Creek level. This means groundwater contributes to the streamflow (Dg) from both banks. While, at cross sections #2 and #3, the surface water level within the creek is higher than groundwater levels on the right and left banks, indicating recharge from Stoney Creek to groundwater (Isw).

At cross sections #4, #5 and #6, the simulated groundwater level within the creek and on either bank of Stoney Creek are higher than the surface water level in Stoney Creek, meaning that groundwater always contributes to streamflow. It is noted that the Stoney Creek water level was not recorded at cross section #6. The results of the numerical simulations show a similar behaviour compared with the observed data. Although at cross sections #2 and #4 the groundwater levels were simulated to be lower and higher than the Stoney Creek water level, respectively.
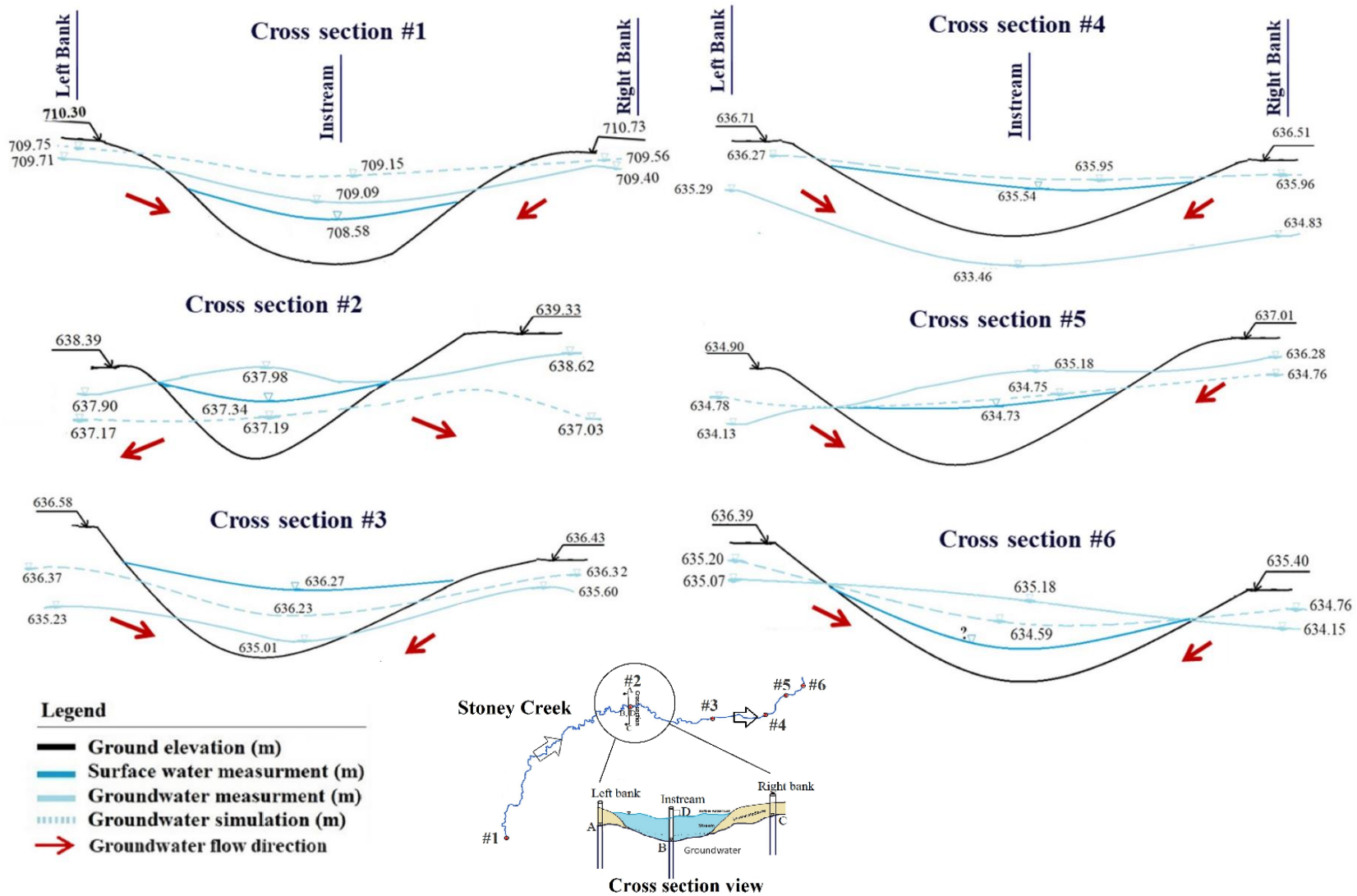
Figure 17. Schematic of observed and simulated water levels along with local groundwater flow direction at each cross section.

Results with the transient model are shown in Figure 18, which displays the time series of simulated groundwater discharge to streamflow in Stoney Creek (Dg) over the three-year modelling period. This figure demonstrates that groundwater discharge varies in different months. From January 2015 to May 2016, Dg gradually decreased, exhibiting a negative trend that is influenced by the precipitation patterns. The highest contribution occurs from January to March 2015 when more than 2.09 MCM is discharged to Stoney Creek from the groundwater system. In 2016, groundwater contribution to streamflow exhibits a significant increase from May to July in response to increased precipitation. It's worth noting that average monthly precipitation in 2016 is wetter (47.33 mm/month) than 2015 (39.02 mm/month) and 2017, which has the lowest monthly precipitation rate (35.95 mm/month) of the three-year modelling period.
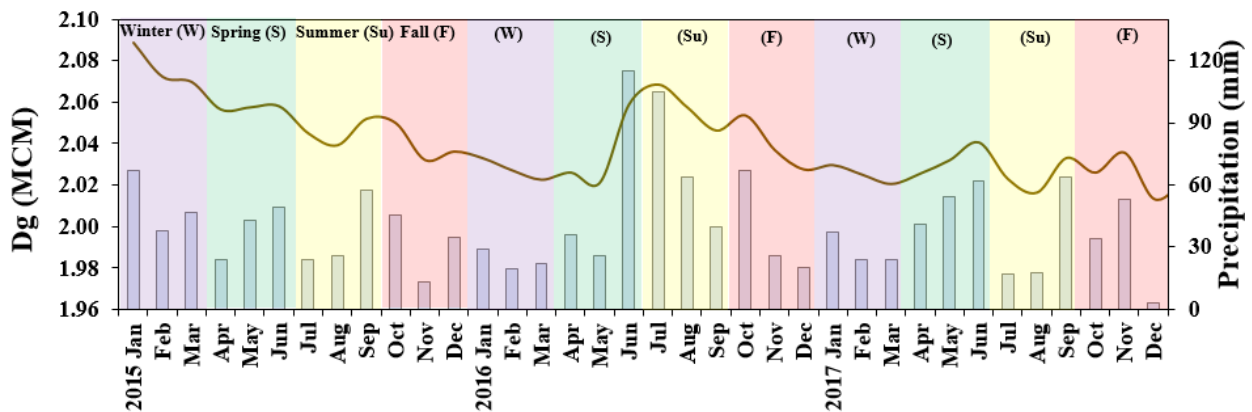
Figure 18. Monthly time series of groundwater contribution (MCM) to streamflow in Stoney Creek and precipitation (mm) from 2015 to 2017.

To assess the contribution of groundwater discharge to streamflow in Stoney Creek, the flow data was analyzed from an active hydrometric station located at the Tachick Lake outlet. Based on the flow data recorded for the year 2016 and 2017, the contribution of groundwater discharge to total flow in Stoney Creek was estimated to be 78.7% and 82.6%, respectively. For instance, in 2017 as a dry year, groundwater contributed most significantly to creek flow during the summer (96.6%), fall (99.5%), and winter (92.8%), while the lowest contribution was estimated in the spring at 41.1%. In July 2017, the Dg was estimated at 2.02 MCM, representing the majority of the recorded creek flow of 2.25 MCM. While in June 2017, when the total creek flow was measured at 7.71 MCM, groundwater discharge was only 2.04 MCM (26%).

The seasonal variation in the contribution of groundwater to creek flow can be attributed to differences in precipitation and runoff patterns. During the summer season, reduced precipitation and significantly decreased surface runoff result in creek flow relying mostly on groundwater discharge. This leads to an increased proportion of groundwater contribution to the overall flow, as demonstrated by the 96.6% contribution observed in 2017. In contrast, during spring, creek flow increases substantially due to snowmelt and seasonal rainfall. This heightened surface water input becomes the dominant source of creek flow, causing groundwater's relative contribution to decrease to 41.1% in the same year. This pattern highlights the inverse relationship between surface water inputs and groundwater contributions to streamflow under varying hydrological conditions.

6.3 Sensitivity Analysis Results

Figure 19 shows the variation of predicted groundwater recharge from Stoney Creek to the aquifer (Isw) from changes in key model parameters over a range of ±25%. Among all parameters, riverbed hydraulic conductivity (K_b) has the greatest effect on model estimates of Isw. For instance, increasing K_b by 25% increases the Isw by 13.6%. The high sensitivity of K_b shows the pivotal role of this parameter affecting the interaction between Stoney Creek and the unconfined aquifer.

The hydraulic conductivity of the confined aquifer (K_{Co}) exhibits the lowest sensitivity on model predictions, for example decreasing K_{Co} by 25% results in a marginal reduction of Isw by 3.9%. The low sensitivity of K_{Co} is mainly attributed to the negligible interaction between Stoney Creek and the confined aquifer system.
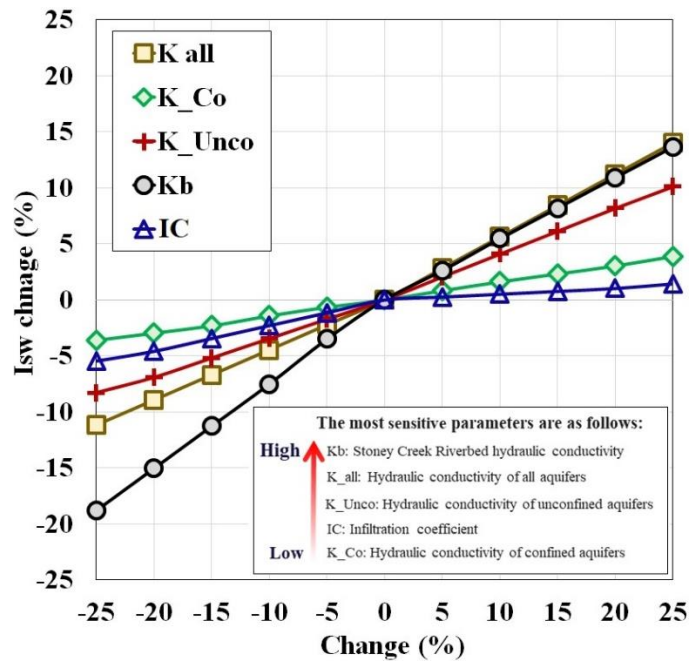
Figure 19. Sensitivity of five key model parameters on model predictions of groundwater recharge from Stoney Creek (K_all: hydraulic conductivity of all aquifers, K_Unco: hydraulic conductivity of unconfined aquifer; IC: infiltration coefficient; K_Co: hydraulic conductivity of confined aquifer; Kb: riverbed hydraulic conductivity).

In addition, Figure 20 shows the predicted spatial distribution of groundwater discharge (Dg) and groundwater recharge (Isw) along Stoney Creek for ±25% changes in riverbed hydraulic conductivity (K_b) and confined aquifer hydraulic conductivity (K_{co}), which had the highest and lowest sensitivity, respectively. Figure 20(a and c) show results for changes in riverbed conductivity (K_b). Decreasing K_b by 25% results in a reduction in groundwater recharge (Isw) from 0.96 to 0.78 MCM/yr (18.8% decrease) and groundwater discharge (Dg) from 24.65 to 22.82 MCM/yr (7.41% decrease). Conversely, increasing K_b by 25% increases groundwater recharge (Isw) by 13.6% (i.e., from 0.96 to 1.09 MCM/yr) and increases groundwater discharge (Dg) by 1.49% (i.e., 25.02 MCM/yr). Results in Figure 20 (b and d) show that changes in confined aquifer conductivity have marginal influence on predicted groundwater-surface water interaction. Decreasing K_{co} by 25%, reduces groundwater recharge (Isw) from 0.96 to 0.92 MCM/yr (3.6% decrease) and insignificantly reduces groundwater discharge (Dg) from 24.65 to 24.74 MCM/yr (0.35% decrease) along Stoney Creek.

(a) -25% K_b

(b) -25% $K_{\_co}$

Legend

Gaining (Dg: 0 to 22.82 MCM/yr)

Losing (Isw is decreased up to 18.8% *)

Legend

Gaining (Dg: 0 to 24.74 MCM/yr)

Losing (Isw is decreased up to 3.6%*)

(c) 25% K_b

(d) 25% $K_{\_co}$

Legend

Gaining (Dg: 0 to 25.02 MCM/yr)

Losing (Isw is increase up to 13.6% *)

Legend

Gaining (Dg: 0 to 24.60 MCM/yr)

Losing (Isw is increase up to 3.9%*)
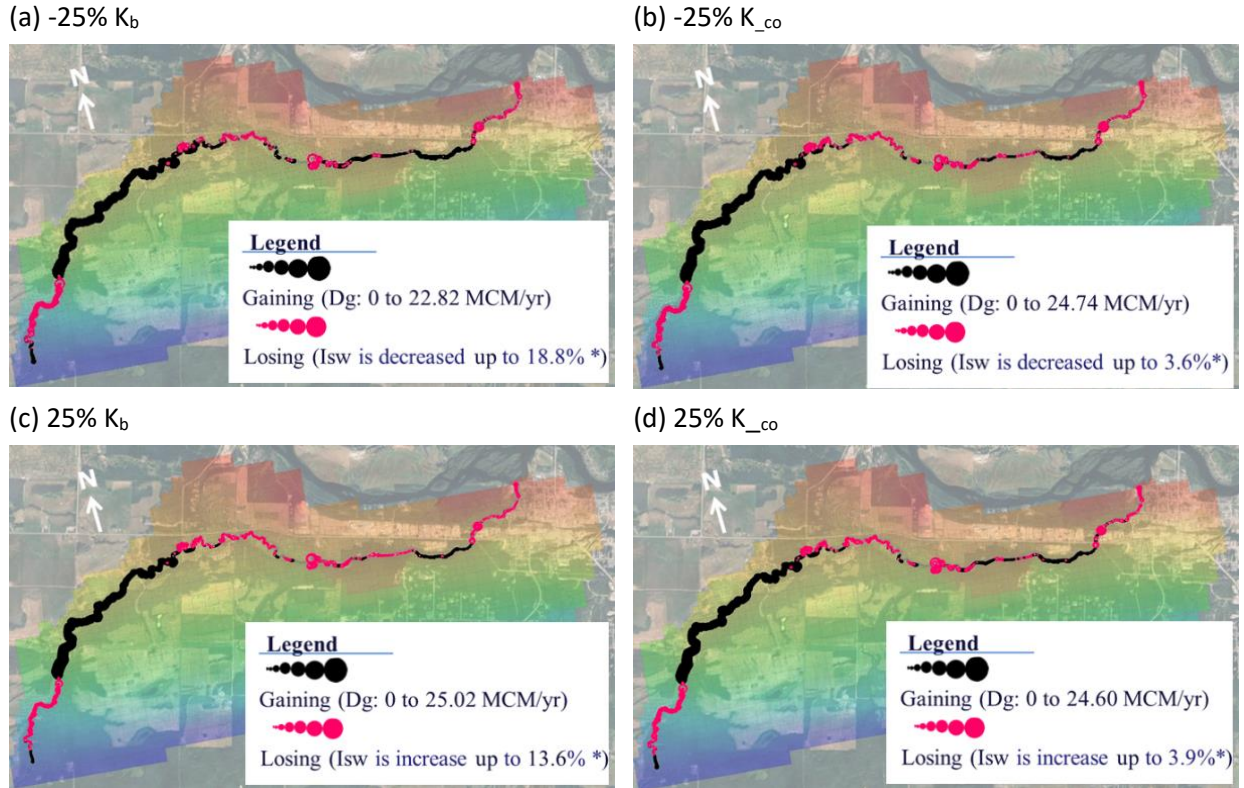
*The percentage changing comparing to the base scenario.

Figure 20. Spatial distribution of predicted groundwater recharge from Stoney Creek under ±25% changes in K_b (a and c) and ±25% changes in $K_{\_co}$ (b and d).

6.4 Groundwater Management Scenarios

The influence of groundwater pumping, including total withdrawal volume and regional groundwater levels, on groundwater-surface interaction in Stoney Creek are discussed in the following sections.

6.4.1 Scenarios MS1 and MS2

In scenarios MS1 and MS2, it is assumed that the groundwater level at the southern and northern boundaries of the study area decreases by 2 m. This scenario was defined because we hypothesize that the future development and population growth, and the associated increase in groundwater demand will lead to a decrease in regional groundwater levels. The northern boundary is closer to Stoney Creek, therefore, water level changes in this area are expected to have more impact on groundwater discharge (Dg) compared to the southern boundary, which is located further from Stoney Creek. Therefore, these two boundaries were analyzed separately instead of decreasing them at the same time.

Table 13 shows the predicted change in groundwater discharge to Stoney Creek (in Dg) due to groundwater level decline at the northern and southern boundaries. In segment 1-2, Dg decreased by 1.9% due to the groundwater level decline at the northern boundary, while a slightly greater reduction in Dg (i.e., 3.7%) was predicted from groundwater level decline at the southern boundary. In segment 2-3, Dg decreased by 35.1% due to lower groundwater levels along the northern boundary groundwater level, but in contrast to segment 1-2, a more modest reduction of Dg (i.e., 11.3%) was predicted from groundwater level decline along the southern boundary. Segments 3-4, 4-5, and 5-6 all follow a similar trend as segment 2-3, showing groundwater level decline along the northern boundary has a greater

effect on groundwater discharge to Stoney Creek than groundwater declines along the southern boundary.

Table 13 shows the largest impacts on groundwater discharge occurred in segments 4-5 and 5-6, which are reaches where Stoney Creek flows through more developed urban areas and areas with a greater concentration of groundwater pumping wells near the northern boundary. Overall, the average reduction in groundwater discharge was about 30% from groundwater level decline along the northern boundary compared to 13% from groundwater level decline along the southern boundary. This emphasizes the need for more focused groundwater management in the northern regions of the Stoney Creek watershed.

Table 13. Changes in groundwater contribution to streamflow (%) induced by groundwater level decrease at northern and southern boundaries.

Segments		Stream reach	Change in groundwater discharge (D_g) to Stoney Creek relative to base case results (%)	
			Northern	Southern
Segment 1-2	Segment 2-3	1-2	1.9	3.7
		2-3	35.1	11.3
		3-4	22.9	10.5
Segment 3-4	Segment 4-5	4-5	35.9	14.1
		5-6	52.4	25.4
		6-end	-	-
Segment 5-6	Segment 6-end	Average	29.6	13

6.4.2 Scenario MS3

For scenario MS3, Figure 21 shows the predicted time series of groundwater discharge (Dg) under different groundwater pumping scenarios including: (1) 10GWP (i.e., 10% increase in groundwater withdrawal), (2) 25GWP, and (3) 50GWP, from 2017 to 2018. For instance, comparison of the base case and a 50% increase in groundwater pumping (50GWP) shows Dg decreased by 0.6% in December 2018.
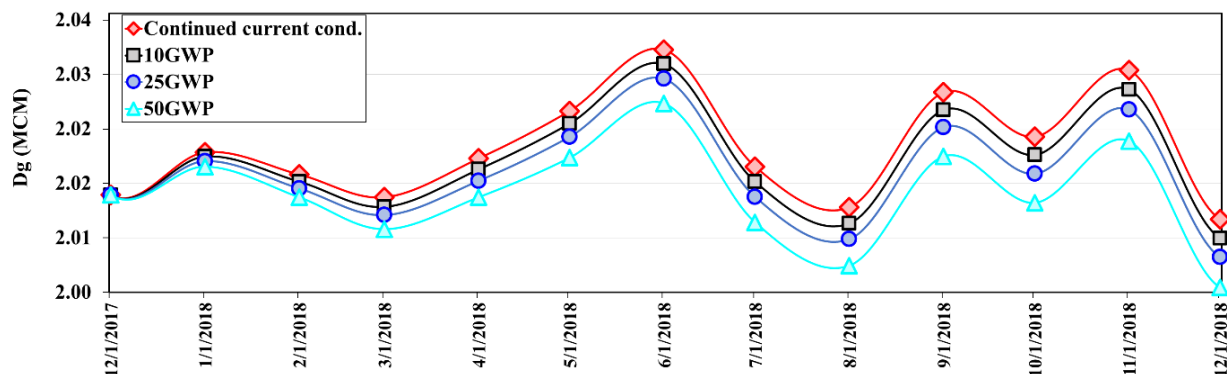

Figure 21. Monthly time series of average groundwater contribution to Stoney Creek in 2018 under different pumping scenarios.

The detailed monthly reduction of Dg is summarized in Table 14. The percentage increases in groundwater withdrawal correspond to the reductions in Dg across these scenarios. For example, the change in groundwater pumping from 10GWP to 25GWP represents a 150% increase in groundwater withdrawal, while the total decrease in Dg changes from 1.5% to 2.3% relative to the base case. In this case, the reduction in Dg is not proportional to the increase in groundwater withdrawal, as the decrease in Dg changes by about 53%. However, comparing the change in groundwater pumping from 25GWP to 50GWP, the corresponding reduction in Dg changes from 2.3% to 4.4% (i.e., ~100% increase), which shows a near proportional relationship at this level of increased withdrawal. Table 14 also shows a seasonal trend where Dg reductions are generally higher in the second half of the year (July to December), especially under higher withdrawal scenarios (50GWP). This further highlights the correspondence between groundwater contributions to Stoney Creek and precipitation patterns.

Table 14 . Change in average groundwater contribution to Stoney Creek (% change relative to the base case results) for different pumping scenarios (year 2018).

MS3	Jan	Feb	Mar	Apr	May	Jun	Jul	Aug	Sep	Oct	Nov	Dec	Sum
10GWP	0.00	0.08	0.16	0.08	0.08	0.20	0.12	0.12	0.12	0.16	0.12	0.25	1.5
25GWP	0.04	0.16	0.16	0.16	0.16	0.20	0.16	0.25	0.24	0.28	0.16	0.37	2.3
50GWP	0.08	0.16	0.24	0.29	0.32	0.40	0.41	0.45	0.45	0.49	0.49	0.61	4.4

The predicted levels of groundwater depletion within both unconfined and confined aquifers are shown in Figure 22 for the 50GWP scenario. The impacts of groundwater pumping on groundwater levels and the associated decrease in groundwater discharge to Stoney Creek depends on the location of pumping wells (e.g., wells completed in unconfined or confined aquifers). Stream depletion resulting from the increased groundwater use in unconfined aquifer wells occurs in less than one month. However, the groundwater level changes are insignificant in the confined aquifers and therefore have little impact to streamflow. The maximum change in groundwater level from increased pumping in the confined aquifer is less than 0.2 cm, whereas it is about 1 cm in the unconfined aquifer. These minimal changes in water levels are due to the low overall pumping rates and comparatively higher levels of groundwater recharge from precipitation. Within the modelling domain, the groundwater recharge rate from precipitation is 1.96 MCM/yr, which is substantially greater than the rate of groundwater withdrawal, which is approximately 0.06 MCM/yr (Table 5) in the 50GWP pumping scenario.

(a)
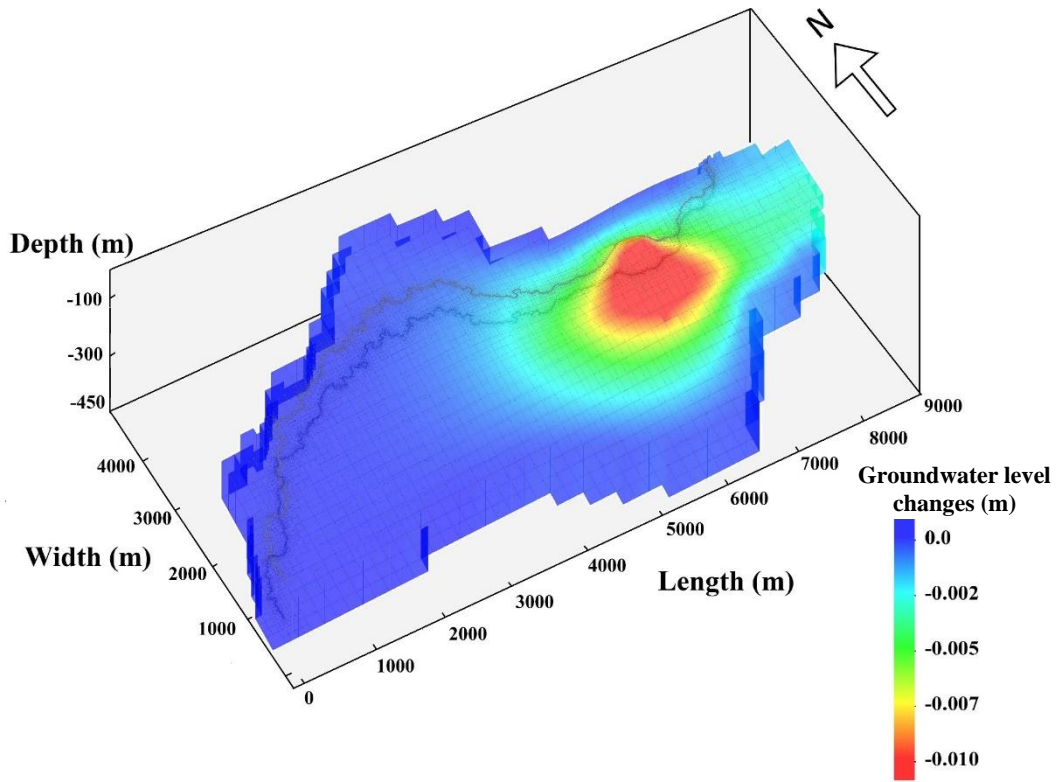
(b)
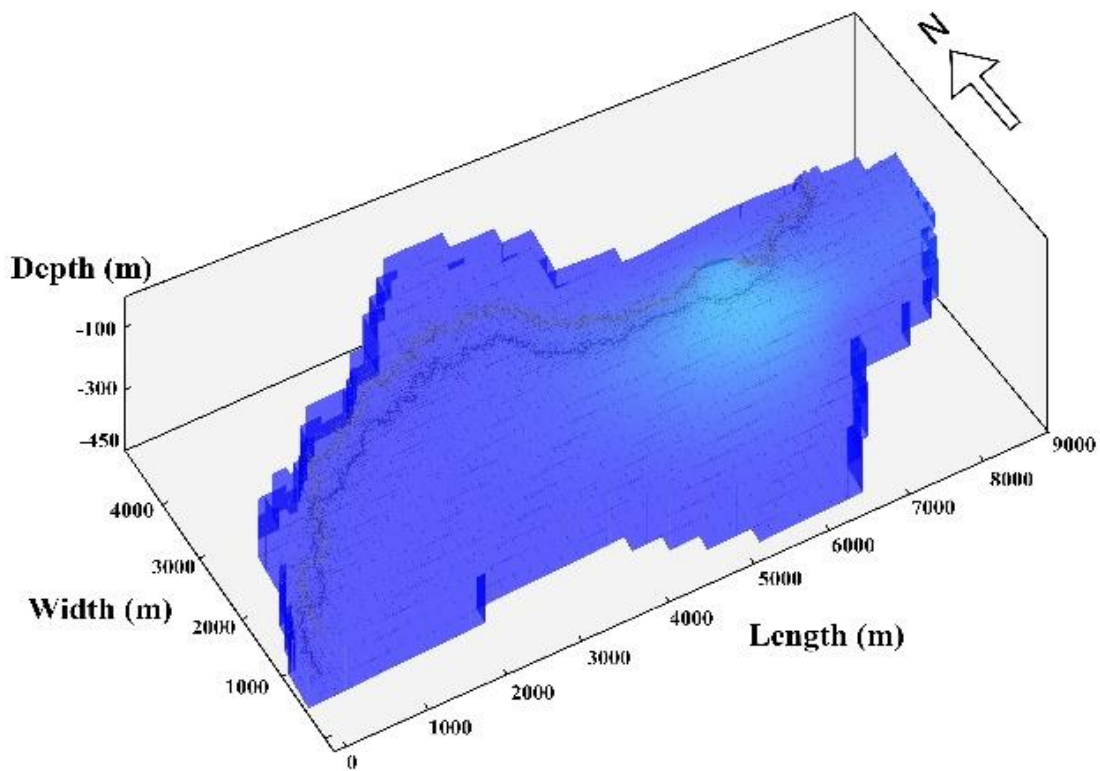
Figure 22. Predicted groundwater level changes relative to the base case results for the 50GWP pumping scenario: (a) unconfined aquifer, (b) confined aquifers.

6.4.3 Scenarios MS4 to MS6

For scenarios MS4, MS5, and MS6, the study area was assumed to be under Wet, Normal, and Dry conditions, which are based on the analysis of precipitation data from the modelling period (Figure 3). In these transient simulations, groundwater use was held at the base level (Table 5) and the modelling period was extended to 2026 (Figure 23). Results for scenario MS4 (Wet conditions) in Figure 23 show groundwater discharge to Stoney Creek (Dg) increases slightly from 24.65 MCM in 2017 to 24.74 MCM by 2026. Similarly, results for scenario MS5 (Normal conditions) show a minimal increase in groundwater discharge from 24.65 MCM to 24.67 MCM (0.06%). These increases indicate that under wet and normal conditions, and without a change in groundwater pumping, the groundwater recharge processes from precipitation effectively enhance or maintain groundwater contributions to surface flow in Stoney Creek.

In scenario MS6, the study area was assumed to be under Dry (reduced rainfall) conditions. Model simulations for this scenario show a reduction of groundwater discharge to Stoney Creek (Dg) from 24.65 MCM to 24.52 MCM by 2026, an overall decrease of about 0.5%. The time series in Figure 23 shows a gradual decline in Dg, reflecting the impact of reduced precipitation recharge during drier conditions. This indicates that in dry years or during times of drought, Stoney Creek is more vulnerable to groundwater depletion, even in the absence of any increase in groundwater pumping.

Figure 23. Time series of groundwater contribution to Stoney Creek under different precipitation and pumping conditions.

6.4.4 Scenario MS7

Scenario MS7 assesses the effects of drier precipitation conditions in the study area combined with increases in groundwater use of 10% to 50% over the base case levels in Table 5. With a 10% increase in groundwater use, groundwater discharge (Dg) gradually decreases 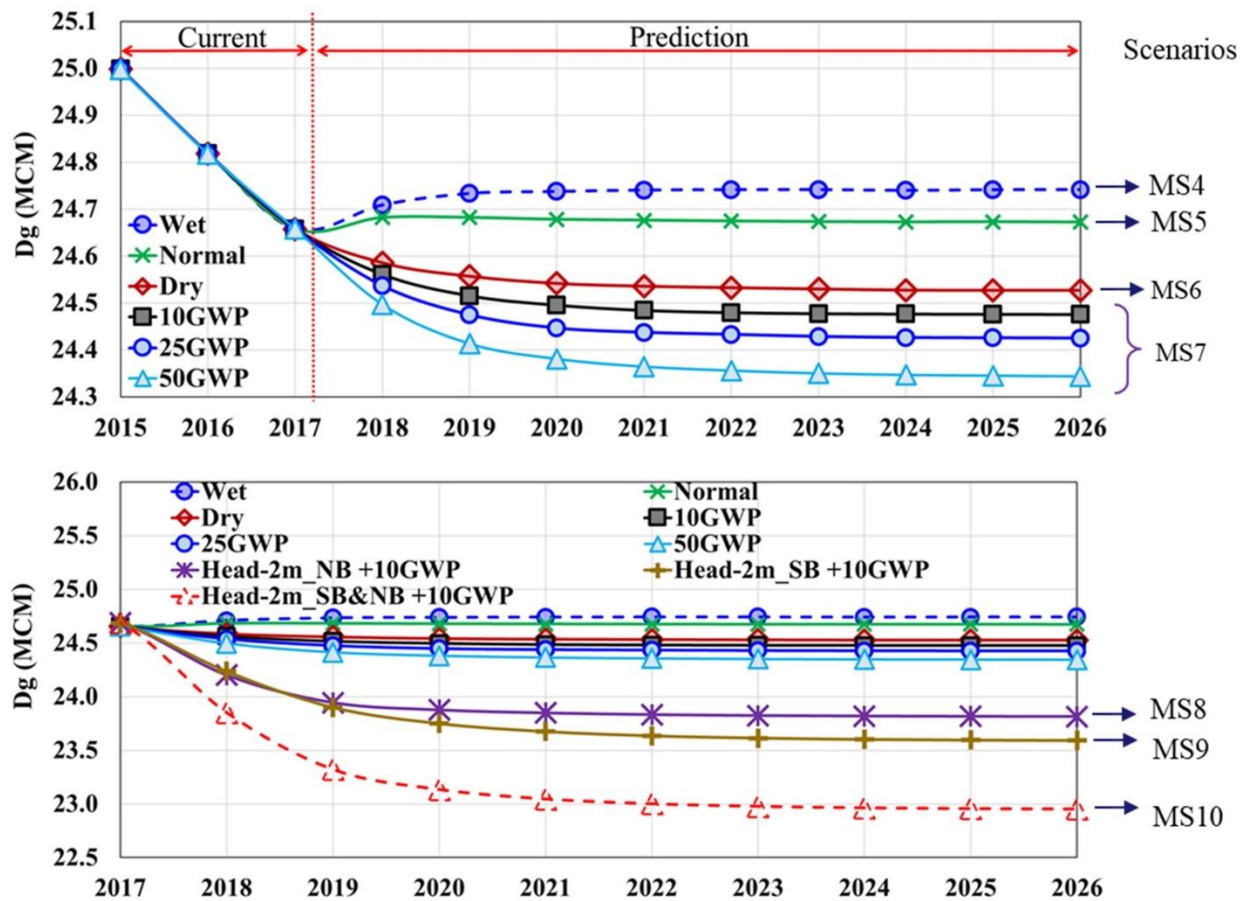to 24.47 MCM by 2026, representing a 0.7% reduction compared to 2017 (Figure 23). The time series plot indicates a steady decline in groundwater contributions to Stoney Creek over the simulation period. Although the reduction is moderate, it suggests that even relatively small increases in groundwater withdrawal can lead to significant decreases in discharge to Stoney Creek (Dg), particularly over extended drier periods. With a 25% increase in groundwater use, the groundwater discharge (Dg) decreases to 24.42 MCM by 2026, a reduction of 0.9% compared to 2017. A 50% increase in groundwater use, further decreases groundwater discharge to 1.3% compared to 2017. This highlights the increased pressure on streamflow depletion in Stoney Creek as pumping rates rise during below average rainfall conditions.

6.4.5 Scenarios MS8 to MS10

Scenarios MS8 to MS10 were defined as cumulative groundwater withdrawal scenarios, entailing a 10% increase in groundwater pumping and a decline in groundwater levels at the boundaries. Scenarios MS8 and MS9 assume that the decline in groundwater levels occur at the northern (MS8) and southern (MS9) boundaries. Scenario MS10 assumes a decline in groundwater levels at both boundaries. As seen in Figure 23, under scenario MS10, the groundwater discharge (D_g) decreased by 7% in 2026 and by 9% in 2035 when the simulation reaches a steady state.

6.5 Risk Analysis

Based on an analysis of groundwater pumping wells and their potential to impact GSI interaction in the modelling domain, Figure 24 schematically illustrates the vulnerability zones of these wells. The vulnerability zones are based on the pumping well location relative to Stoney Creek and on the well depth and aquifer type from which they are pumping. Additionally, the hazard component was quantified using a water level change map, which was calculated based on a 50% increase in groundwater use.

Three general vulnerability zones are defined in Figure 24 and described below. The spatial location of pumping wells and their associated risk levels are shown in the risk map in Figure 25:

- **Very high-risk wells** are located in unconfined aquifers in close proximity to Stoney Creek and demonstrate significant groundwater level changes due to groundwater withdrawal. These rapid changes and the wells' proximity to Stoney Creek can potentially result in rapid, short-term streamflow depletion responses in Stoney Creek from changes in groundwater pumping.
- **Moderate to high-risk wells** are located in unconfined or confined aquifers in relatively close proximity to Stoney Creek. Current pumping rates from these wells produce small to insignificant groundwater level responses, however, substantial increase in pumping rates from these wells could potentially produce a significant streamflow depletion response in Stoney Creek.
- **Low to very low-risk wells** are located in the confined or bedrock aquifers at comparatively larger distances from Stoney Creek, and current pumping rates from these wells produce small to insignificant groundwater level responses.
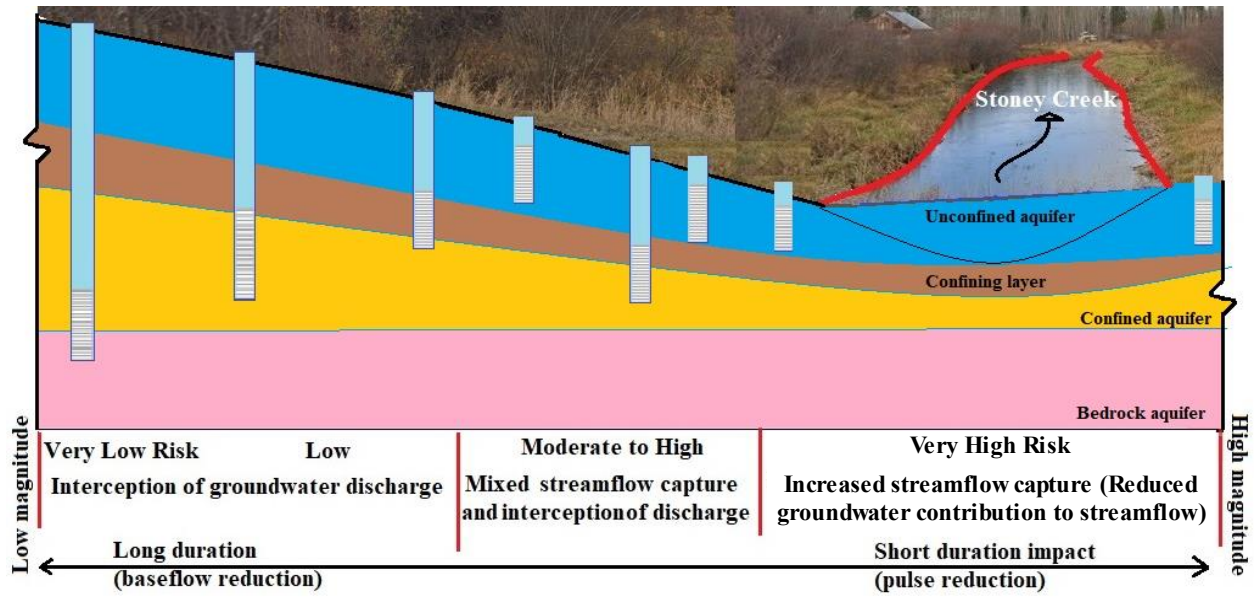
Figure 24. Vulnerability zones of pumping wells based on well depth and location in aquifers in the Stoney Creek watershed.
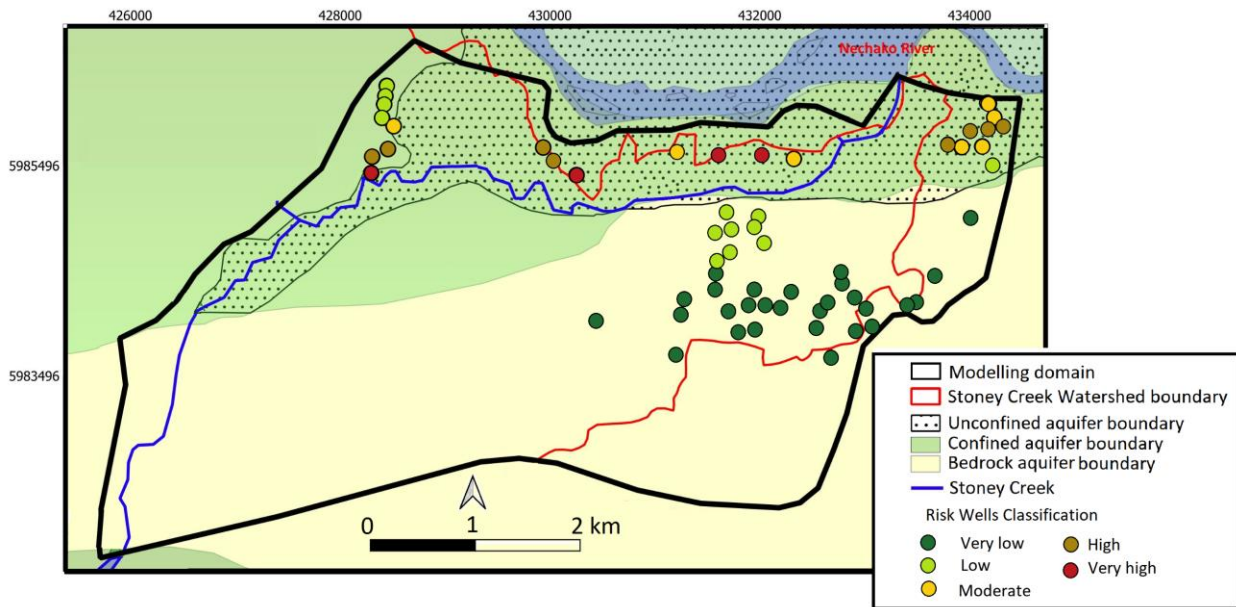

Figure 25. Risk map of pumping wells based on the water level changes, well depth and well location in the different aquifers along Stony Creek

7. CONCLUSION AND RECOMMENDATIONS

7.1 Summary and Key Findings

A conceptual model of groundwater flow in the Stoney Creek watershed was developed using available lithology data. The conceptual model was the basis for development of a 3-D numerical model to simulate groundwater and surface water interaction (GSI) in the lower part of the Stoney Creek watershed. The numerical model was calibrated for steady-state and transient conditions using time-dependent groundwater level (in piezometers) and Stoney Creek water level measurements collected along six stream transects from 2015 to 2017. Static groundwater level data (i.e., measured at the time of drilling) available from the GWELLS database and recorded in both unconfined and confined aquifer wells were also used for model calibration. The piezometric water level and static water level data were weighted equally during the calibration procedure. Calibration parameters (total 15) included the hydraulic conductivity and anisotropy ratio of the modelled geologic units, the streambed hydraulic conductivity, and infiltration coefficients based on different land use classes in the study area. A sensitivity analysis was conducted to evaluate the influence of the main modelling parameters on the simulation outcomes. The calibrated model was used to assess the influence of different management (pumping), climate, and groundwater level scenarios on groundwater-surface water interaction and streamflow depletion in Stoney Creek. Finally, a streamflow depletion risk map for existing wells in the watershed was developed on the basis of well location and simulated pumping responses.

The key findings and conclusions of this study based on the integrated assessments are:

- Groundwater discharge is a significant source of streamflow in Stoney Creek. The base case simulation results demonstrate that groundwater discharge to Stoney Creek ranges from 0.01 to 23.6 million cubic meters per year (MCM/yr) depending on the stream sections. Much of the groundwater discharge occurs in stream reach 1-2 in the upper portion of the modelled domain. In the northern part of the study area (stream reach 4-5, close to urban areas in Vanderhoof), average groundwater discharge to Stoney Creek was estimated to be 0.13 MCM/yr, which was balanced by groundwater recharge from Stoney Creek to the underlying aquifer of 0.11 MCM/yr. Future increases in groundwater use near higher demand urban areas can potentially disrupt the balance in groundwater-surface water interaction along this stream reach.

- The time series of simulated groundwater discharge shows an association between streamflow response and precipitation. Groundwater discharge to Stoney Creek increases quickly during periods of above average precipitation, gradually diminishing during periods of average and below average precipitation. This indicates that longer-term changes in precipitation patterns can affect groundwater-surface water responses along Stoney Creek.

- Riverbed hydraulic conductivity (K_b) and the hydraulic conductivity of unconfined aquifers are the most sensitive and important parameters for simulation of groundwater-surface water interaction in Stoney Creek. This suggests that data collection efforts focused on these parameters could help to improve model calibration and performance. The least sensitive model parameter was the hydraulic conductivity of confined aquifer ($K_{\_Co}$).

- Specified head boundary conditions along the southern and northern boundaries of the model domain have a significant influence on the simulation of groundwater discharge to Stoney Creek (Scenarios MS1 and MS2). Current and future groundwater levels along these boundaries are uncertain due to the lack of monitoring information and the potential for future development and population growth to decrease regional groundwater levels. A 2 m decline in groundwater levels along the northern boundary resulted in a 30% reduction in predicted groundwater discharge to Stoney Creek, compared to a 13% reduction for similar groundwater level decline

along the southern boundary. The most sensitive and impacted stream sections in the model simulations were segments 4-5 and 5-6 close to the northern boundary. These results emphasize the need for more focused groundwater management in the northern regions of the study domain. Establishing groundwater level monitoring wells in these regions could help to improve model calibration, reliability, and confidence in model performance, as well as to support regional groundwater resource management.

- Increases in groundwater use can reduce groundwater discharge to Stoney Creek (Scenario MS3). The calibrated transient groundwater provides a means to assess the effect of changes in groundwater pumping on streamflow depletion in Stoney Creek. A 50% increase in groundwater pumping reduced groundwater discharge by 0.6% in December 2018. This relatively small effect at the regional scale reflects the substantial volumetric difference of groundwater pumping in comparison to groundwater recharge. However, we note that significant impacts from groundwater pumping on streamflow depletion can occur at more reach specific or local scales, particularly from larger pumping wells or well fields. With further model calibration and testing, the model developed in this study can provide a tool for allocation staff to assess impacts from large scale groundwater use applications.

- Climate patterns affect simulation results of groundwater discharge to Stoney Creek (Scenarios MS4, MS5, MS6). The simulation of extended periods of above average precipitation resulted in an increase in groundwater discharge from 24.65 MCM in 2017 to 24.74 MCM by 2026. Conversely, under dry conditions with extended periods of below average precipitation, the simulated groundwater discharge decreased from 24.65 MCM to 24.52 MCM by 2026, resulting in an overall reduction of about 0.5%. With ongoing model development and testing, more representative climate-change scenarios can be simulated in the groundwater model to assess the longer-term effects of climate-change on groundwater system response and to support longer-term resource planning and management.

- The numerical groundwater model provides a means to assess groundwater system response to multiple stresses. For example, scenario MS7 assessed the effects from increased pumping during dry (drought) conditions, and scenarios MS8 to MS10 assessed the cumulative effects of increased pumping and regional groundwater level decline. In each of these cases, simulation results showed that cumulative effects from multiple stresses further exacerbates the effects on reduction in groundwater discharge to Stoney Creek. With further development, calibration and verification, the numerical groundwater model can serve as a comprehensive tool for supporting long-term groundwater resource management.

- A risk analysis of simulated groundwater pumping impacts on groundwater discharge to Stoney Creek identified and mapped vulnerability zones of groundwater pumping, which can assist water officers in the adjudication of groundwater licence applications. The vulnerability map showed wells classified as very high-risk are located in unconfined aquifers in close proximity to Stoney Creek and experienced significant water level changes due to groundwater withdrawal. These changes could potentially reduce groundwater contribution to Stoney Creek in the short term. Wells classified as moderate to high-risk, despite having insignificant water level changes, were located in unconfined or confined aquifers and may potentially impact Stoney Creek in the long term. Wells classified as low to very low-risk are located in the confined or bedrock aquifers and demonstrate insignificant water level changes from pumping.

7.2 Limitations and Recommendations

The scope of this project did not include the assessment of impacts from a combination of various factors, such as drought conditions and land use changes. The understanding of cumulative impacts and the interaction among various factors are more meaningful for informed watershed management and groundwater allocation decisions.

The previously installed piezometers (six cross sections along the creek) in the SCW can measure water levels, however some of them were damaged and located on private lands with difficult access. Therefore, the piezometers need to be repaired, reinstalled or relocated for future work. The pipe diameters for data loggers need to be considered based on the type of data logger. For example, one type of data logger requires a 1-inch diameter pipe, while another type can be installed with a 3/4-inch diameter pipe.

The surface water flow and level measurements at different locations along Stoney Creek are recommended to develop a more accurate GSI numerical model. In this way, the developed numerical model can be refined to simulate surface water flow routing and to investigate the effects of groundwater withdrawals on the Stoney Creek level (see Delottier et al., 2024).

The numerical modelling indicated that the GSI mainly occurred between the unconfined aquifer and the surface water in the creek, but the hydraulic conductivity of the unconfined aquifer was not measured. These data were estimated using literature values or based on pumping test results in confined aquifers outside the Stoney Creek watershed (e.g., Observation Well 516 and 455). To further refine the numerical model and to achieve a more accurate understanding of the GSI, it is of essential importance to measure the hydraulic conductivity of the unconfined aquifers.

REFERENCES

Aghbelagh, Y.B., Li, J., and Yin, J. 2018. Surface Water and Groundwater Interactions in the Stoney Creek Watershed: Insights from Numerical Groundwater Flow Modelling, Province of British Columbia, Victoria.

Angen, J. J., Hart, C. J. R., Kim, R. S. Rahimi, S. 2018. Geology and mineral potential of the trek area, northern interior plateau, central British Columbia, parts of 1:250,000 NTS sheets 093b, c, f and g. Geoscience BC report 2018-12. The University of British Columbia - mineral deposit research unit.

Ayenew, T., Demlie, M., Wohnlich, S. 2008. Application of numerical modelling for groundwater flow system analysis in the Akaki catchment, central Ethiopia. Mathematical geosciences, 40, 887-906.

Baawaain, M.S., A.M. Al-Futaisi, A. Ebrahimi, and H. Omidvarborna. 2018. Characterizing leachate contamination in a landfill site using Time Domain Electromagnetic (TDEM) imaging. Journal of Applied Geophysics 151: 73-81.

Bailey, R. T., Park, S., Bieger, K., Arnold, J. G., Allen, P. M. 2020. Enhancing SWAT+ simulation of groundwater flow and groundwater-surface water interactions using MODFLOW routines. Environmental Modelling & Software, 126, 104660.

Bailey, R. T., Tasdighi, A., Park, S., Tavakoli-Kivi, S., Abitew, T., Jeong, J., Worqlul, A. W. 2021. APEX-MODFLOW: A New integrated model to simulate hydrological processes in watershed systems. Environmental Modelling & Software, 143, 105093.

Balbarini, N., Boon, W. M., Nicolajsen, E., Nordbotten, J. M., Bjerg, P. L., Binning, P. J. 2017. A 3-D numerical model of the influence of meanders on groundwater discharge to a gaining stream in an unconfined sandy aquifer. Journal of Hydrology, 552, 168-181.

Banerjee, D., Ganguly, S. 2023. A review on the research advances in groundwater–surface water interaction with an overview of the phenomenon. Water, 15(8), 1552.

Beck, H. E., Zimmermann, N. E., McVicar, T. R., Vergopolan, N., Berg, A., Wood, E. F. 2018. Present and future Köppen-Geiger climate classification maps at 1-km resolution. Scientific data, 5(1), 1-12.

Bordet, E., Mihalynuk, M. G., Hart, C. J. R. Sanchez, M. 2013. Three-dimensional thickness model for the eocene volcanic sequence, chilcotin and nechako plateaus, central British Columbia. Geoscience BC summary of activities, 2013, 43-52

Briggs, M.A., C.B. Dawson, C.L. Holmquist-Johnson, K.H. Williams, and J.W. Lane. 2019. Efficient hydrogeological characterization of remote stream corridors using drones. Hydrological Processes 33, no. 2: 316-319. https://doi.org/10.1002/hyp.13332

Chow, R., Frind, M. E., Frind, E. O., Jones, J. P., Sousa, M. R., Rudolph, D. L., Nowak, W. 2016. Delineating baseflow contribution areas for streams–A model and methods comparison. Journal of contaminant hydrology, 195, 11-22.

Chow, V. T., Maidment, D. R., Mays, L. W. 1988. *Applied Hydrology*, McGraw-Hill, New York.

Clague, J. J. 1981. Late Quaternary Geology and Geochronology of British Columbia Part 2: Summary and Discussion of Radiocarbon-Dated Quaternary History. Geological Survey of Canada, paper 80-35, 41 pages.

Clague, J. J. 1988. Quaternary Stratigraphy and History, Quesnel, British Columbia. Géographie Physique et Quaternaire, 42, 279-288.

Clague, J. J. 2000. Recognizing Order in Chaotic Sequences of Quaternary Sediments in the Canadian Cordillera. Quaternary International, 68-71, 29-38

Coluccio, K. 2018. A comparison of methods for estimating groundwater-surface water interactions in braided rivers, Masters of Water Resource Management, University of Canterbury, Christchurch, New Zealand.

Coluccio, K., Morgan, L. K. 2019. A review of methods for measuring groundwater–surface water exchange in braided rivers. Hydrology and Earth System Sciences, 23(10), 4397-4417.

Cui, G., Su, X., Zheng, S., Tong, S., Jiang, M. 2024. Hydrological and biogeochemical processes controlling riparian groundwater quantity and quality during riverbank filtration. Environmental Pollution, 350, 124020.

Cui, Y., Miller, D., Schiarizza, P. Diakow, L. J. 2017. British Columbia Digital Geology. British Columbia Geological Survey Open File. British Columbia Ministry of Energy, Mines and Petroleum Resources.

De Stefano, L., Petersen-Perlman, J. D., Sproles, E. A., Eynard, J., Wolf, A. T. 2017. Assessment of transboundary river basins for potential hydro-political tensions. Global Environmental Change, 45, 35-46.

Deb, P., Kiem, A.S., Willgoose, G.R. 2019. Mechanisms influencing non-stationarity in rainfall-runoff relationships in southeast Australia. Journal of Hydrology, 571, 749–764.

Delleur, J.W. 2007. The Handbook of Groundwater Engineering, 2nd Edition, CRC Press LLC.

Delottier, H., Schilling, O. S., Therrien, R. 2024. Assessing the impact of surface water and groundwater interactions for regional-scale simulations of water table elevation. Journal of Hydrology, 639, Article 131641.

Fang, J., Al-Hamdan, M. Z., O'Reilly, A. M., Ozeren, Y., Rigby, J. R. 2024. A three-dimensional numerical model for variably saturated groundwater flow using meshless weak-strong form method. Environmental Modelling & Software, Article 105982.

Ferbey, T. 2011. Till Geochemistry of the Colleymount Map Area (093l/01), West-Central British Columbia. Geoscience BC.

Fetter, C.W. 2001. *Applied Hydrogeology*. Prentice Hall, Englewood Cliffs.

Foks, S.S., J.P. Raffensperger, C.A. Penn, and J.M. Driscoll. 2019. Estimation of base flow by optimal hydrograph separation for the conterminous United States and implications for national-extent hydrologic models. Water 11: 1629. https://doi.org/10.3390/w11081629

Forstner, T., Gleeson, T., Borrett, L., Allen, D.M., Wei, M., and Baye, A. 2018. Mapping aquifer stress, groundwater recharge, groundwater use, and the contribution of groundwater to environmental flows for unconfined aquifers across British Columbia. Water Science Series, WSS2018-04. Prov. B.C., Victoria.

Freeze, R.A. and Cherry, J.A., 1979. *Groundwater*, Prentice Hall, Englewood Cliffs, 604 pp.

Gebere, A., Kawo, N. S., Karuppannan, S., Hordofa, A. T., Paron, P. 2021. Numerical modelling of groundwater flow system in the Modjo River catchment, Central Ethiopia. Modelling Earth Systems and Environment, 7(4), 2501-2515.

Geoscience BC. 2009. Quest project - geology, map 2009-4-1, 1:500,000. Geoscience BC

Ghysels, G.; Anibas, C.; Awol, H.; Tolche, A.D.; Schneidewind, U. 2021. Huysmans, M. The Significance of Vertical and Lateral Groundwater–Surface Water Exchange Fluxes in Riverbeds and Riverbanks: Comparing 1D Analytical Flux Estimates with 3D Groundwater Modeling. Water, 13, 306.

Hammett, S., Day-Lewis, F. D., Trottier, B., Barlow, P. M., Briggs, M. A., Delin, G., Werkema, D. D. 2022. GW/SW-MST: A groundwater/surface-water method selection tool. Groundwater, 60(6), 784-791.

Harbaugh, A. W. 2005. MODFLOW-2005, the US Geological Survey modular ground-water model: the ground-water flow process (Vol. 6). Reston, VA, USA: US Department of the Interior, US Geological Survey.

Hinnell, A.C., T. Lengyel, S. Funk, J.J Clague and Z.M. Hammond. 2020. Vanderhoof and Houston Aquifer Mapping and Hydrostratigraphic Characterization, Water Science Series, WSS2020-07. Province of British Columbia, Victoria.

Hirshfield, F. 2011. Kiskatinaw River Surface and Ground water monitoring network: Field protocol, hydrometric advice and Year 1 results. Technical report, University of Northern BC.

Hirshfield, F. 2013. Kiskatinaw River surface water monitoring network: A summary of methodology and rating curve development, (June). Technical report, University of Northern BC.

Jackson, K. 2020. Investigating Local and Valley-Scale Controls on the Spatial Patterning of Preferential Groundwater Discharge. MS Graduate Thesis, Department of Natural Resources and the Environment, University of Connecticut.

Jafari, T., Kiem, A. S., Javadi, S., Nakamura, T., Nishida, K., 2021. Fully integrated numerical simulation of surface water-groundwater interactions using SWAT-MODFLOW with an improved calibration tool. Journal of Hydrology: Regional Studies, 35, 100822.

Joo, J., Tian, Y. 2021. Impact of Stream-Groundwater Interactions on Peak Streamflow in the Floods. Hydrology, 8(3), 141.

Karamouz, M., Mahmoodzadeh, D., Oude Essink, G. H. 2020. A risk-based groundwater modelling framework in coastal aquifers: a case study on Long Island, New York, USA. Hydrogeology Journal, 28(7).

Karki, R., Srivastava, P., Kalin, L., Mitra, S., Singh, S. 2021. Assessment of impact in groundwater levels and stream-aquifer interaction due to increased groundwater withdrawal in the lower Apalachicola-

Chattahoochee-Flint (ACF) River Basin using MODFLOW. Journal of Hydrology: Regional Studies, 34, 100802.

Kasahara, T., Wondzell, S. M. 2003. Geomorphic controls on hyporheic exchange flow in mountain streams. Water Resources Research, 39(1), SBH-3.

Kebede, S.; Charles, K.; Godfrey, S.; MacDonald, A.; Taylor, R.G. 2021. Regional-scale interactions between groundwater and surface water under changing aridity: Evidence from the River Awash Basin, Ethiopia. Hydrol. Sci. J, 66, 450–463.

Ketabchi, H., Mahmoodzadeh, D., Valipour, E., Saadi, T. 2024. Uncertainty-based analysis of water balance components: a semi-arid groundwater-dependent and data-scarce area, Iran. Environment, Development and Sustainability, 26, pp 31511–31537 .

Khan, H. H., Khan, A., 2019. Groundwater and surface water interaction. Chap 14 in GIS and Geostatistical techniques for Groundwater Science (V. Senapathi et al., eds), 22, Elsevier, https://doi.org/10.1016/B978-0-12-815413-7.00014-6.

Lambert, P.M., Marston, T., Kimball, B.A., and Stolp, B.J. 2011. Assessment of groundwater/surface- water interaction and simulation of potential streamflow depletion induced by groundwater withdrawal, Uinta River near Roosevelt, Utah: U.S. Geological Survey Scientific Investigations Report 2011–5044, 47 p.

Lane, J.W., M.A. Briggs, P.K. Maurya, E.A. White, J.B., Pedersen ,E. Auken, N. Terry, B. Minsley, W. Kress, D.R. LeBlanc, R. Adams, and C.D. Johnson. 2020. Characterizing the diverse hydrogeology underlying rivers and estuaries using new floating transient electromagnetic methodology, Science of the Total Environment, v. 740, 140074

Larned, S. T., Unwin, M. J., and Boustead, N. C. 2015. Ecological dynamics in the riverine aquifers of a gaining and losing river, Freshwater Science, 34, 245-262,

Li, M.; Liang, X.; Xiao, C.; Cao, Y. 2020. Quantitative evaluation of groundwater–surface water interactions: Application of cumulative exchange fluxes method. Water, 12, 259.

Li, Z., Xiao, K., Li, Y., Pan, F., Li, H., Zheng, Y., Liu, Y. 2024. Surface water-groundwater interactions drive the spatial variability of dissolved heavy metals and interfacial fluxes in mangrove intertidal zones. Journal of Hydrology, Article 130884.

Mahmoodzadeh, D., Karamouz, M. 2022. A hydroeconomic simulation-optimization framework to assess the cooperative game theory in coastal groundwater management. Journal of Water Resources Planning and Management, 148(1), 04021092.

Mahmoodzadeh, D., Ketabchi, H., Ataie-Ashtiani, B., Simmons, C. T. 2014. Conceptualization of a fresh groundwater lens influenced by climate change: A modelling study of an arid-region island in the Persian Gulf, Iran. Journal of Hydrology, 519, 399-413.

Mahmoodzadeh, D., Yin, J., Li, J. 2023. Conceptualization of surface water and groundwater interactions in Stoney Creek Watershed, British Columbia, Canada. PEOPLE 2023 International Conference – Collaborative Solutions to Environmental Problems under Climate Change on August 7-11 in Montreal, Canada (Oral presentation).

Mahmoodzadeh, D., Yin, J., Li, J. 2024. Conceptualization of surface water and groundwater interactions in Stoney Creek Watershed, British Columbia, Canada. CSCE 2024 Conference on June 5-7 in Niagara Falls, Canada (Oral presentation).

May, R., Mazlan, N. S. B. 2014. Numerical simulation of the effect of heavy groundwater abstraction on groundwater–surface water interaction in Langat Basin, Selangor, Malaysia. Environmental earth sciences, 71, 1239-1248.

McDonald, M.G., and A.W. Harbaugh 1988. A Modular Three-Dimensional Finite-Difference Ground-Water Flow Model: U.S. Geological Survey Techniques of Water-Resource Investigations, Book 6, Chapter A1, pp. 586

Mohtashami, S., Eliasson, L., Hansson, L., Willén, E., Thierfelder, T., Nordfjell, T. 2022. Evaluating the effect of DEM resolution on performance of cartographic depth-to-water maps, for planning logging operations. International Journal of Applied Earth Observation and Geoinformation, 108, 102728.

Moore, E.M., K.E. Jackson, A.B. Haynes, A.M. Helton, and M.A. Briggs. 2020. Thermal infrared images of groundwater discharge zones in the Farmington and Housatonic River watersheds (Connecticut and Massachusetts, 2019). U.S. Geological Survey data release.

Naganna, S. R., Deka, P. C., Ch, S., Hansen, W. F. 2017. Factors influencing streambed hydraulic conductivity and their implications on stream–aquifer interaction: a conceptual review. Environmental Science and Pollution Research, 24, 24765-24789.

Rajaeian, S., Ketabchi, H., Ebadi, T. 2024. Investigation on quantitative and qualitative changes of groundwater resources using MODFLOW and MT3DMS: a case study of Hashtgerd aquifer, Iran. Environment, Development and Sustainability, 26(2), 4679-4704.

Rau, G.C., V.E.A. Post, M. Shanafield, T. Krekeler, E.W. Banks, and P. Blum. 2019. Error in hydraulic head and gradient time-series measurements: a quantitative appraisal. Hydrology and Earth System Science, 23(9): 3603-3629.

Rumsey, C.A., M.P. Miller, and G.A. Sexstone. 2020. Relating hydroclimatic change to streamflow, baseflow, and hydrologic partitioning in the Upper Rio Grande Basin, 1980 to 2015. Journal of Hydrology, 584.

Sacco, D. A., Ward, B. C., Lian, O. B., Maynard, D. E. Geertsema, M. 2017. Quaternary Geology of Part of the Mcleod Lake Map Area (NTS 093J), Central British Columbia: Lithostratigraphy, Glacial History, And Chronology. Canadian Journal of Earth Sciences, 54, 1063-1084.

Sadat-Noori, M., Anibas, C., Andersen, M.S., Glamore, W. 2021. A comparison of radon, heat tracer and head gradient methods to quantify surface water-groundwater exchange in a tidal wetland (Kooragang Island, Newcastle, Australia). Journal of Hydrology. 2021,598, 126281.

Saha, G. C., Li, J., Thring, R.W., Hirshfield, F. and Paul, S.S. 2017. Temporal Dynamics of Groundwater-Surface Water Interaction Under the Effects of Climate Change: A Case Study in the Kiskatinaw River Watershed, Canada. Journal of Hydrology, 551, 440-452.

Sanchez, J., Etebari, B. 2019. Evaluating Stream Depletions in Small Watersheds and Headwaters of California Stream Depletion Risk Assessment Framework & Tools (sDRAFT). Presentation file, California Water Board.

Sanz, D., Castaño, S., Cassiraga, E., Sahuquillo, A., Gómez-Alday, J. J., Peña, S., Calera, A. 2011. Modelling aquifer-river interactions under the influence of groundwater abstraction in the Mancha Oriental System (SE Spain). Hydrogeology Journal, 19(2), 475.

Singh, M. K., Ghosh, S. 2022. River Aquifer Interaction Modelling for the Waterlogged Aquifer and Sustainable Groundwater Irrigation along River Flood Plain. Journal of the Geological Society of India, 98(9), 1271-1282.

Stefania, G., Rotiroti, M., Fumagalli, M., Simonetto, F., Capodaglio, P., Zanotti, C., Bonomi, T. 2018. Modeling groundwater/surface-water interactions in an Alpine valley (the Aosta Plain, NW Italy): the effect of groundwater abstraction on surface-water resources. Hydrogeology Journal, 26(1), 147-162.

Strasser, D., Lensing, H. J., Nuber, T., Richter, D., Frank, S., Goeppert, N., Goldscheider, N. 2015. Improved geohydraulic characterization of river bed sediments based on freeze-core sampling–development and evaluation of a new measurement approach. Journal of Hydrology, 527, 133-141.

Struik, L. C., Macintyre, D. G. Williams, S. P. 2007. Nechako Natmap Project: A Digital Suite of Geoscience Information for Central British Columbia. Geological Survey of Canada, Open File 5623.

Stumpf, A. J. 2008. Till Geochemistry and Clast Lithology Studies of The Bulkley River Valley, West- Central British Columbia (Parts of NTS 093l). Geoscience BC Report

Stumpf, A. J., Broster, B. E. Levson, V. M. 2004. Glacial Stratigraphy of The Bulkley River Region: A Depositional Framework for The Late Pleistocene in Central British Columbia. Geographie Physique Et Quaternaire, 58, 217-228

Thomas, E.O. Effect of temperature on D.O. and T.D.S. 2021. A measure of Ground and Surface Water Interaction. Water Sci., 35, 11–21

Tran, Q. D., Ni, C. F., Lee, I. H., Truong, M. H., Liu, C. J. 2020. Numerical modelling of surface water and groundwater interactions induced by complex fluvial landforms and human activities in the Pingtung plain groundwater basin, Taiwan. Applied Sciences, 10(20), 7152.

Valett, H.M., R.W. Sheibley. 2009. Ground Water and Surface Water Interaction, In Encyclopedia of Inland Waters, Edited by Gene E. Likens, Academic Press

Waseem, M., Kachholz, F., Klehr, W., Tränckner, J. 2020. Suitability of a Coupled Hydrologic and Hydraulic Model to Simulate SurfaceWater and Groundwater Hydrology in a Typical North-Eastern Germany Lowland Catchment. Appl. Sci, 10, 1281.

Weatherup, S. Struik, L. C. 1996. Vanderhoof Metamorphic Complex and Surrounding Rocks, Central British Columbia. Geological Survey of Canada - Current Research 1996-A, 63-70.

Yihdego, Y., and Becht, R. 2013. Simulation of lake–aquifer interaction at Lake Naivasha, Kenya using a three-dimensional flow model with the high conductivity technique and a DEM with bathymetry. Journal of Hydrology, 503, 111-122.

Zaremehrjardy, M., Victor, J., Park, S., Smerdon, B., Alessi, D. S., Faramarzi, M. 2022. Assessment of snowmelt and groundwater-surface water dynamics in mountains, foothills, and plains regions in northern latitudes. Journal of Hydrology, 606, 127449.

Zhou, D., Zhang, Y., Gianni, G., Lichtner, P., Engelhardt, I. 2018. Numerical modelling of stream– aquifer interaction: Quantifying the impact of transient streambed permeability and aquifer heterogeneity. Hydrological Processes, 32(14), 2279-2292.

Zhou, Y., Li, W. 2011. A Review of Regional Groundwater Flow Modelling. Geoscience Frontiers, 2(2), 205-214.

Zhou, Y., Liang, X., Ma, E., Chen, K., Zhang, J., Zhang, Y. K. 2023. Effect of Unsaturated Flow on Groundwater-River Interactions Induced by Flood Event in Riparian Zone. Journal of Hydrology, 620, 129405.

Zlotnik V.A., A. Ward, J.W. Harvey, L.K. Lautz, D.O. Rosenberry, and P. Brunner. 2016. Groundwater-surface Water Interactions. In Handbook of Groundwater Engineering, ed. John H Cushman and Daniel M. Tartakovsky, 237-288. Boca Raton: CRC Press.